

10-2019

Analysis of Connectivity in EMG Signals to Examine Neural Correlations in Muscular Activation of Lower Leg Muscles for Postural Stability

Diana McCrumb
Grand Valley State University

Follow this and additional works at: <https://scholarworks.gvsu.edu/theses>



Part of the [Kinesiology Commons](#), and the [Neuroscience and Neurobiology Commons](#)

ScholarWorks Citation

McCrumb, Diana, "Analysis of Connectivity in EMG Signals to Examine Neural Correlations in Muscular Activation of Lower Leg Muscles for Postural Stability" (2019). *Masters Theses*. 959.
<https://scholarworks.gvsu.edu/theses/959>

This Thesis is brought to you for free and open access by the Graduate Research and Creative Practice at ScholarWorks@GVSU. It has been accepted for inclusion in Masters Theses by an authorized administrator of ScholarWorks@GVSU. For more information, please contact scholarworks@gvsu.edu.

**Analysis of Connectivity in EMG Signals to Examine Neural Correlations in Muscular
Activation of Lower Leg Muscles for Postural Stability**

Diana McCrumb

A Thesis Submitted to the Graduate Faculty of

GRAND VALLEY STATE UNIVERSITY

In

Partial Fulfillment of the Requirements

For the Degree of

Master of Science in Engineering, Biomedical Engineering

Padnos College of Engineering and Computing

August 2019

Acknowledgement

I would like to thank my thesis advisor Dr. Rhodes for her invaluable guidance and expertise throughout my time in the graduate program as well as the undergraduate program. Her knowledge has helped me immensely in completing my degree requirements.

I would like to thank the members of my committee, Dr. Alderink and Dr. Lee, who have given their time and expertise in mentoring me through this process. Their knowledge has been invaluable in the completion of my thesis. I am very thankful to Dr. Alderink for giving his time and dedication in helping me become familiar with the biomechanics lab.

I would like to thank all the participants of this study for giving their valuable time to participate.

Finally, I would like to thank my friends and family for their constant support throughout my academic career. Without them I would not have achieved as much as I have today.

Abstract

In quiet standing the central nervous systems implements a pre-programmed ankle strategy of postural control to maintain upright balance and stability. This strategy is comprised of a synchronized common neural drive being delivered to synergistically grouped muscles. In this study connectivity between EMG signals of unilateral and bilateral homologous muscle pairs, of the lower legs, during various standing balance conditions was evaluated using magnitude squared coherence (MSC) and mutual information (MI). The leg muscles of interest were the tibialis anterior (TA), medial gastrocnemius (MG), and the soleus (S) of both legs. MSC is a linear measure of the phase relation between two signals in the frequency domain. MI is an information theoretic measure of the amount of information two signals have in common. Both MSC and MI were analyzed in the delta (0.5 – 4 Hz), theta (4 – 8 Hz), alpha (8 – 13 Hz), beta (13 – 30 Hz), and gamma (30 – 100 Hz) neural frequency bands for feet together and feet tandem, with eyes open and eyes closed conditions. Both MSC and MI found that overall connectivity was highest in the delta band followed by the theta band. Connectivity in the beta and lower gamma bands (30 – 60 Hz) was influenced by standing balance condition and indicative of a neural drive originating from the motor cortex. Instability was evaluated by comparing less stable standing conditions with a baseline eyes open, feet together stance. Changes in connectivity in the beta and gamma bands were found be most significant in the muscle pairs of the back leg of tandem stance regardless of foot dominance. MI was found to be a better connectivity analysis method by identifying significance of increased connectivity in the agonistic muscle pair between the MG:S, the antagonistic muscle pair between TA:S, and all the bilateral homologous muscle pairs. MSC was only able to identify the MG:S muscle pair as significant. The results of this study provided insight into the neural mechanism of postural control and presented an alternative connectivity analysis method of MI.

Table of Contents

Acknowledgement	3
Abstract.....	4
List of Tables	7
List of Figures	8
Abbreviations	10
Chapter 1. Introduction	11
1.1. Introduction.....	11
1.2. Purpose	13
1.3. Scope.....	13
1.4. Assumptions	14
1.5. Hypothesis.....	14
1.6. Significance.....	15
1.7. Definitions	16
Chapter 2. Manuscript	17
Abstract.....	17
2.1. Introduction.....	18
2.2. Methods	20
2.2.1. Participants	20
2.2.2. Procedure.....	21
2.2.3. Data Acquisition.....	21
2.2.4. Data Analysis.....	22
2.3. Results	26
2.3.1. Magnitude Squared Coherence	26

2.3.2.	Mutual Information	39
2.4.	Discussion	52
2.4.1.	Connectivity	52
2.4.2.	Comparison of Connectivity Analysis Methods	54
2.4.3.	Limitations and Future Consideration.....	55
2.5.	Conclusion	55
Chapter 3.	Extended Review of Literature and Extended Methodology.....	57
3.1.	Extended Review of Literature	57
3.1.1.	Motor Control.....	57
3.1.2.	Neural Control Theories	58
3.1.3.	Human Balance and Postural Control.....	60
3.1.4.	Quiet Standing	64
3.1.5.	Connectivity	67
3.2.	Extended Methodology.....	69
3.2.1.	Participants	69
3.2.2.	Experimental Procedure.....	69
3.2.3.	Data Acquisition.....	71
3.2.4.	Data Analysis.....	74
Appendix A.	Figures	80
Appendix B.	Code	84
Bibliography	88

List of Tables

Table 2.1: Quiet standing balance conditions	21
Table 2.2: Neural frequency bands	22
Table 2.3: Muscle pairs.....	23
Table 3.1: Neural frequency bands and their known origin	60
Table 3.2: Plantarflexor (P) and dorsiflexor (D) muscles of the lower legs.....	63
Table 3.3: Participant characteristics.....	69
Table 3.4: Quieting standing balance conditions.....	70

List of Figures

Figure 2.1: Functional block diagram of the data analysis process.....	23
Figure 2.2: Average and standard error of the mean MSC in the delta band	27
Figure 2.3: Average and standard error of the mean MSC in the theta band.....	28
Figure 2.4: Average and standard error of the mean MSC in the alpha band	29
Figure 2.5: Average and standard error of the mean MSC in the beta band	30
Figure 2.6: Average and standard error of the mean MSC in the lower gamma band.....	31
Figure 2.7: Average and standard error of the mean MSC in the upper gamma band	32
Figure 2.8: Results of Dunnett’s two-sided post-hoc t-test for multiple comparisons against baseline (EOFT) condition for significant MSC in the alpha band.....	35
Figure 2.9: Results of Dunnett’s two-sided post-hoc t-test for multiple comparisons against baseline (EOFT) condition for significant MSC in the beta band.....	36
Figure 2.10: Results of Dunnett’s two-sided post-hoc t-test for multiple comparisons against baseline (EOFT) condition for significant MSC in the lower gamma band	37
Figure 2.11: Results of Dunnett’s two-sided post-hoc t-test for multiple comparisons against baseline (EOFT) condition for significant MSC in the upper gamma band.....	38
Figure 2.12: Average and standard error of the mean MI in the delta band	40
Figure 2.13: Average and standard error of the mean MI in the theta band	41
Figure 2.14: Average and standard error of the mean MI in the alpha band	42
Figure 2.15: Average and standard error of the mean MI in the beta band	43
Figure 2.16: Average and standard error of the mean MI in the lower gamma band	44
Figure 2.17: Average and standard error of the mean MI in the upper gamma band	45

Figure 2.18: Results of Dunnett’s two-sided post-hoc t-test for multiple comparisons against baseline (EOFT) condition for significant MI in the alpha band	47
Figure 2.19: Results of Dunnett’s two-sided post-hoc t-test for multiple comparisons against baseline (EOFT) condition for significant MI in the beta band	48
Figure 2.20: Results of Dunnett’s two-sided post-hoc t-test for multiple comparisons against baseline (EOFT) condition for significant MI in the lower gamma band.....	49
Figure 2.21: Results of Dunnett’s two-sided post-hoc t-test for multiple comparisons against baseline (EOFT) condition for significant MI in the upper gamma band	50
Figure 3.1: the motor unit.....	57
Figure 3.2: Simple conceptual model of postural control.....	62
Figure 3.3: Postural control strategies	63
Figure 3.4: 4-stage functional assessment balance test positions [36].....	65
Figure 3.5: Inverted pendulum models and their postural control strategies adapted from [1]	65
Figure 3.6: Feet orientation	71
Figure 3.7: Pre-amplifier placement.....	72
Figure 3.8: Modified Full-Body Plug-in-Gait model.....	73
Figure A.1: Results of Dunnett’s two-sided post-hoc t-test for multiple comparisons against baseline (EOFT) condition for significant MSC in the delta band.....	80
Figure A.2: Results of Dunnett’s two-sided post-hoc t-test for multiple comparisons against baseline (EOFT) condition for significant MSC in the theta band	81
Figure A.3: Results of Dunnett’s two-sided post-hoc t-test for multiple comparisons against baseline (EOFT) condition for significant MI in the delta band	82
Figure A.4: Results of Dunnett’s two-sided post-hoc t-test for multiple comparisons against baseline (EOFT) condition for significant MI in the theta band.....	83

Abbreviations

BOS – base of support

CNS – central nervous system

COM – center of mass

COP – center of pressure

DsOF – degrees of freedom

EC – eyes closed

EO – eyes open

FT – feet together

EMG – electromyography

MG – medial gastrocnemius

MI – mutual information

M-mode – muscle mode

MSC – magnitude squared coherence

MU – motor unit

MUAP – motor unit action potential

S – soleus

sEMG – surface electromyography

SIP – single inverted pendulum model

TA – tibialis anterior

TanDB – tandem dominant foot in back

TanDF – tandem dominant foot in front

Chapter 1. Introduction

1.1. Introduction

Human balance refers to a state of equilibrium where a body's center of pressure (COP) oscillates about its center of mass (COM) that is within the area of the base of support (BOS), made up of the feet to prevent a fall [1]–[3]. Humans are inherently unstable bipeds that need a continuously acting postural control system to maintain balance and stability due to their relatively large COM and relatively small BOS [1], [4]. Postural control is defined as a learned complex motor skill, used by the central nervous system (CNS), that engages the interaction of multiple sensorimotor processes to maintain, achieve, or restore a state of balance to the musculoskeletal system [2], [4]. The actual neural mechanism used in the organization and coordination of musculoskeletal movement is not entirely known. The focus of this study is to better understand the neural mechanism of postural control implemented by the CNS during quiet standing.

The single inverted pendulum (SIP) biomechanical model has been widely adapted to quantify the ankle strategy, or ankle movements, present during the maintenance of balance in quiet stance [1], [5]. The ankle strategy requires active coordination of multiple lower leg muscles; each muscle requires the activation and coordination of thousands of individual motor units (MUs). It has been suggested that the ankle strategy is a pre-programmed movement strategy, specific to postural control, implemented by the CNS to rectify a loss of balance and stability [1], [6], [7]. However, the exact musculoskeletal elements and how they are synchronized are yet to be fully understood. This knowledge gap in postural control, and by extension motor control, arise from the degrees of freedom (DOFs) problem introduced by Bernstein [8]. Simply put, the CNS has control over more movement elements than possible movement tasks. In terms of postural control, the ankle strategy could be coordinated by an infinite number of possible coordination patterns or DOFs. It has been

suggested that the CNS simplifies the number of possible effective DOFs by coupling muscles to be controlled in conjunction [8], [9]. How muscles are coupled, either anatomically (mechanical) or functionally (neural), has been the source of numerous research studies [7], [9]–[23]. In literature, groups of muscles that are synchronously activated are defined as muscle synergies; and the signal that synchronously activates these muscles is called a common neural drive [7], [10], [24], [25].

The concept of synchronized common neural drives has been widely observed between the CNS and postural control muscles as a way to simplify individual muscle activation [7], [9]–[23]. These studies implemented intermuscular coherence analysis on electromyography (EMG) signals to assess the presence of synchronized common neural drives. Distinct neural frequency band oscillations from the CNS to postural muscles are discernable from the surface EMG signals. Intermuscular coherence (EMG-EMG) in the neural frequency bands has been indicative of the neural origin of synchronized common neural drives specific postural muscle pairs [10]–[23]. While there appears to be a consensus that common neural drives are implemented, the muscle synergies that receive the drives are not agreed upon. Synergies, thus far, have been functionally determined or anatomically determined by intermuscular coherence analysis. Only one study has theorized that both anatomical and functional connectivity contributes to how the muscles of the musculoskeletal system were modularly organized [9].

Coherence is a connectivity analysis method that is limited by linearity. Thus, by using coherence, all of these studies have only looked at the linear characteristics of EMG. Non-linear characteristics do exist in EMG signals [26], [27]. Mutual information (MI) is an information theoretic measure of connectivity that is not limited by linear dependence. It estimates how much information can be obtained of one signal from the observation of another. This study was conducted to compare functional connectivity analysis results of intermuscular coherence and MI with respect to foot dominance and quiet standing balance tasks.

1.2. Purpose

The aim of this study was to examine connectivity between EMG signals of various pairs of lower leg muscles, in the neural frequency bands, during various quiet standing conditions of normal healthy adults. The lower leg muscles of interest were the tibialis anterior (TA), medial gastrocnemius (MG), and the soleus (S) of the right (R) and left (L) legs. These muscles were chosen due to their involvement in facilitating ankle movement. The goal was to assess the role of foot dominance as it pertains to maintaining balance and stability as well as compare connectivity analysis methods of intermuscular coherence and MI. Understanding connectivity between muscle pairs will help to provide insight into the neural mechanism implemented by the CNS for postural control.

1.3. Scope

This study analyzed and compared how well connectivity analysis methods of intermuscular coherence, using magnitude squared coherence (MSC), and MI will convey synchronous muscle activation between ankle muscles (TA, GM and S) involved in the ankle strategy of postural control. This study also examined the role of foot dominance as it applies to muscular activation during various quiet standing balancing conditions. A total of six balancing conditions were examined: feet together (FT), feet tandem with the dominant foot in back (TanDB), and feet tandem with dominant foot in front (TanDF) for both eyes open (EO) and eyes closed (EC). Surface EMG signals were collected at the L/RTA, L/RMG, and L/RS. Connectivity between unilateral and bilateral homologous muscle pairs were examined in the delta (0.5 – 4 Hz), theta (4 – 8 Hz), alpha (8 – 13 Hz), beta (13 – 30 Hz), and gamma (30 – 100 Hz) neural frequency bands. A single MSC and MI value for each frequency band was estimated for each muscle pair during each standing balance condition. One-way ANOVAs compared the change in connectivity between the most stable (baseline, EOFT) standing balance condition with the other, less stable, conditions for both MSC

and MI. The use of MSC and MI may provide insight in the relationship between synchronized common neural drive and the muscular synergies of postural control.

1.4. Assumptions

For the purpose of this study it was assumed that all humans have a predefined underlying postural control system from birth that can be improved upon based on their expectations, goals, and prior experiences. Therefore, it was assumed that each individual has a postural control system unique to them, but their underlying postural control system, before learning, would be similar. Each individual was statistically analyzed against themselves due to possibility of learned differences in their postural control systems. Eyes open, feet together was assumed to be the most stable condition for all other quiet standing conditions to compare against. It was also assumed that foot dominance would play a role in the necessary muscular activation during various quiet standing balancing tasks. The final assumption was that muscles that are neither unilateral nor bilateral homologous will not show connectivity information and thus will not be compared.

1.5. Hypothesis

Previous studies found that high coherence between muscle pairs, in the neural frequency bands, is indicative of shared structural connections or synchronized common neural drives [10]–[23]. Therefore, it was hypothesized that high coherence in certain neural frequency bands was indicative of the neural origin of the synchronized common neural drive. It was also hypothesized that high coherence between muscle pairs will give insight on how the postural muscle synergies, involved in ankle strategy, are organized. With respect to connectivity analysis methods between the various muscle pairs of the lower legs it was hypothesized that MI would display better functional and anatomical connectivity than MSC due to being able to analyze both linear and non-linear

characteristics of EMG. A previous study showed that coherence was significant between the RMG and RS muscle pair and increased from higher to lower neural frequency bands during various standing balance conditions of right foot dominate (RFD) participants [28]. This protocol focused on balance stances of FT and TanDB for both EO and EC. The results of this study suggested that foot dominance may play a role in coherence strength of muscle pairs in the same leg. For the present research it was hypothesized that alternating the front foot in tandem stance will alter the strength of connectivity in the dominant and non-dominant foot.

1.6. Significance

Assessing the significance of intermuscular connectivity during quiet standing balance tasks provides a means for evaluating the presences of synchronized common neural drives in neural frequency bands. The goal of this study was to provide further confirmation that distinct correlations in certain frequency bands during various quiet standing balance tasks, for normal healthy adults, is indicative of the neural origin of the synchronized common neural drive. Another goal was to provide a more accurate alternative to coherence in MI for assessing connectivity. By gaining a better understanding of the neural mechanism implemented by postural control during quiet standing will provide a suitable baseline reference to compare against when evaluating various clinical balance implications. These implications could be related to aging, diseases of the CNS, neurological conditions, and traumatic brain injuries can be developed.

1.7. Definitions

Common neural drive: theory that the CNS uses a single neural drive to simultaneously synchronize the activation of multiple muscles rather than one individual muscle

Functional connectivity: when groups of muscles share a common neural drive

Anatomical connectivity: when groups of muscles share a physical connection

Synergy: a group of muscles that are synchronized by a common neural drive

Coherence: measure of the linear phase correlation between two signals in the frequency domain

Mutual Information: measure of the amount of information shared between two signals

Chapter 2. Manuscript

Abstract

In quiet standing the central nervous systems implements a pre-programmed ankle strategy of postural control to maintain upright balance and stability. This strategy is comprised of a synchronized common neural drive being delivered to synergistically grouped muscles. In this study connectivity between EMG signals of unilateral and bilateral homologous muscle pairs, of the lower legs, during various standing balance conditions was evaluated using magnitude squared coherence (MSC) and mutual information (MI). The leg muscles of interest were the tibialis anterior (TA), medial gastrocnemius (MG), and the soleus (S) of both legs. MSC is a linear measure of the phase relation between two signals in the frequency domain. MI is an information theoretic measure of the amount of information two signals have in common. Both MSC and MI were analyzed in the delta (0.5 – 4 Hz), theta (4 – 8 Hz), alpha (8 – 13 Hz), beta (13 – 30 Hz), and gamma (30 – 100 Hz) neural frequency bands for feet together and feet tandem, with eyes open and eyes closed conditions. Both MSC and MI found that overall connectivity was highest in the delta band followed by the theta band. Connectivity in the beta and lower gamma bands (30 – 60 Hz) was influenced by standing balance condition and indicative of a neural drive originating from the motor cortex. Instability was evaluated by comparing less stable standing conditions with a baseline eyes open, feet together stance. Changes in connectivity in the beta and gamma bands were found be most significant in the muscle pairs of the back leg of tandem stance regardless of foot dominance. MI was found to be a better connectivity analysis method by identifying significance of increased connectivity in the agonistic muscle pair between the MG:S, the antagonistic muscle pair between TA:S, and all the bilateral homologous muscle pairs. MSC was only able to identify the MG:S muscle pair as significant. The results of this study provided insight into the neural mechanism of postural control and presented an alternative connectivity analysis method of MI.

2.1. Introduction

Humans are inherently unstable bipeds that require a continuously acting postural control system to maintain balance and stability. Balance is defined as the state of equilibrium where an individual's center of pressure (COP) oscillates about their center of mass (COM) that is within the area of the base of support (BOS), made up of their feet and ankles to prevent a fall [1]–[3]. Postural control is defined as a learned complex motor skill implemented by the central nervous system (CNS) to promote balance and stability, of the musculoskeletal system, derived from an individual's expectations, goals, cognitive factors, and prior experiences [3], [4]. This system engages the interaction of multisensory inputs from the visual, vestibular, and somatosensory systems to produce the necessary coordinated motor outputs needed to generate musculoskeletal movement [1], [24]. The actual neural mechanism used in the organization and coordination of musculoskeletal motor control is not entirely known. The focus of this study is to better understand the neural control mechanism of musculoskeletal movement as it relates to postural control during quiet standing.

The single inverted pendulum (SIP) biomechanical model has been widely recognized as an acceptable model to quantify the prominent plantar/dorsiflexion ankle movement strategy that is present during the maintenance of balance in quiet stance [1], [5]. Movement of each individual plantar/dorsiflexor muscle requires the activation and coordination of thousands of individual motor units (MUs). How the CNS is able to coordinate these numerous activations to perform a specific movement task has been the subject of numerous motor control studies [6], [20], [25]–[27]. The degrees of freedom (DOFs) problem was introduced to explain how the CNS has control over more musculoskeletal elements than possible musculoskeletal movements [25]. A one-to-one correspondence between a specific motor task and coordination pattern, of the musculoskeletal elements, cannot exist within the DOFs problem. Redundancy arises from the infinite number of possible coordination patterns that are capable of generating the same movement task. It has been

suggested that the CNS simplifies individual MU activation by implementing a common neural drive to a motoneuron pool consisting of all the motor neurons required to innervate a single muscle [6]. Current studies support the existence of common neural drives as the neural mechanism dictating motor control, however instead of motor pool activation these studies suggest the activation of synergistical organized groups of muscles [6]–[20], [26], [27]. In the diverse field of motor control the term synergy has carried various connotations that are often not synonymous between various research approaches [27]. Muscle synergies have been grouped by functional and anatomical connectivity.

Numerous studies have implemented electromyography (EMG) and intermuscular (EMG-EMG) coherence to analyze functional connectivity in underlying traces of synchronized correlated neural drive oscillations, from the CNS, within and between postural leg muscles [6]–[19]. Coherence measures the linearity of the phase relation between two signals in the frequency domain. These studies found that high coherence, at a specific frequency, between unilateral and bilateral homologous postural muscle pairs is indicative of a synchronized common neural drive. The frequency at which these neural drives oscillate at is characteristic of their signal origin in the brain. High coherence in the type of muscle pairs may provide insight as to how the muscles of musculoskeletal system are synergistically grouped.

Although coherence has been widely used to quantify functional connectivity between muscle pairs that belong to a defined synergy it is limited by the assumption of linear association. If two signals contain similar non-linear characteristics coherence will be 0, which indicates no correlation, even though their non-linear characteristics are related [28]. EMG signals should not be assumed to be entirely linear due to being derived from the nonlinear transformation of signal inputs to outputs that occur within the motor neuron [22]. Mutual information (MI) is an information theoretic measure of connectivity that estimates how much information one signal contains about

another and is not limited by this assumption of linear dependence. MI quantifies the reduction of uncertainty of future values of one signal due to the knowledge of another signal [29].

This study was conducted to examine connectivity from EMG signals between various unilateral and bilateral homologous muscle pairs of the lower legs in the neural frequency bands during various quiet standing conditions with respect to foot dominance of normal healthy adults. The goal of this study is to assess the role of foot dominance in balance maintenance as well as compare connectivity between muscle pairs in the frequency domain using coherence and MI. Comparing functional connectivity results of coherence and MI will add valuable insight to existing theories of the neural mechanism related to the maintenance of balance and postural stability used by the CNS.

2.2. Methods

2.2.1. Participants

Six healthy young adults (2 male and 4 females), between the ages of 18 – 34, and of varying physical activity level voluntarily provided their signed informed consent prior to participating in this study. All subjects were considered healthy with no history of neurological or muscular disorders or injuries. Foot dominance was identified based on each subject's assumed preference. If preference was unknown subjects were asked to identify their preferred leg to kick a ball. A follow up task of standing on one leg was implemented for subjects who were unable to determine a preference from the previously asked questions. This study was approved by the Human Research Review Committee, Institutional Review Board, Office of Research Compliance and Integrity, at Grand Valley State University (18-246-H).

2.2.2. Procedure

Subjects completed five 30 second trials of six different balancing conditions (listed in Table 2.1) starting with eyes open, feet together (EOFT) to quantify a stable baseline to compare the other balance conditions to.

Table 2.1: Quiet standing balance conditions

Condition	Order	Description
EOFT	1	Eyes open, feet together
ECFT	2	Eyes closed, feet together
EOTanDB	3	Eyes open, feet tandem, dominant foot in back
ECTanDB	4	Eyes closed, feet tandem, dominant foot in back
EOTanDF	5	Eyes open, feet tandem, dominant foot in front
ECTanDF	6	Eyes closed, feet tandem, dominant foot in front

A 30-second break was implemented between trials and a 2-minute break between each condition. Conditions were completed in the order they were listed across all subjects based on foot dominance. Balance tasks were performed barefoot and arms were positioned so that the index finger pointed towards the shoulders and elbows pulled in.

2.2.3. Data Acquisition

Surface EMG signals, motion trajectories, and COP oscillations were synchronized using Vicon NEXUS motion capture software v2.8 (Oxford Metrics, Oxford, UK). Only EMG data were used for further analysis.

2.2.3.1. Surface EMG

Surface EMG was recorded at the left (L) and right (R) tibialis anterior (TA), medial gastrocnemius (MG), and soleus (S) of the lower legs using MA-411 pre-amplifiers interfaced with the MA300-XVI EMG patient unit acquisition system (Motion Lab Systems Inc., Baton Rouge, LA) at a 1200 Hz sampling frequency. These muscles were chosen due to their prominent role in ankle

movement. The patient unit implemented a 500 Hz low-pass anti-aliasing filter on the raw EMG before transmitting it to desktop unit where the signal was further filtered with a 10 Hz high pass filter.

2.2.3.2. *Motion Capture and Force Plates*

A total of 16 Vicon MX cameras (Oxford Metrics, Oxford, UK) were used to track movement trajectories of a modified Full-Body Plug-in-Gait (FB PiG) model during quiet standing balance tasks at a sampling frequency of 120 Hz. The modified model included the addition of a fifth metatarsal (5thMet) and medial knee markers. Two floor-embedded AMTI (Advanced Mechanical Technology Inc., Watertown, MA) force plates, oriented one directly in front of the other, were used to measure ground reactions during quiet standing balance tasks at a sampling frequency of 1200 Hz. The use of the second force plate was implemented to measure separate ground reactions present when feet were positioned in tandem stance.

2.2.4. **Data Analysis**

All recorded EMG signals were analyzed in the frequency domain using MATLAB R2018a (The MathWorks, Natick, MA) for the following neural frequency bands (Table 2.2) and muscle pairs (Table 2.3) to observe the presence of synchronized correlated neural drives. The data analysis process carried out in this section is illustrated in Figure 2.1.

Table 2.2: Neural frequency bands of interest

Band	Range (Hz)
Delta	0 – 4
Theta	4 – 8
Alpha	8 – 13
Beta	13 – 30
Lower Gamma	30 – 60
Upper Gamma	60 – 100

Table 2.3: Muscle pairs of interest

Left Unilateral	Right Unilateral	Bilateral Homologous
LTA:LMG	RTA:RMG	LTA:RTA
LTA:LS	RTA:RS	LMG:RMG
LMG:LS	RMG:RS	LS:RS

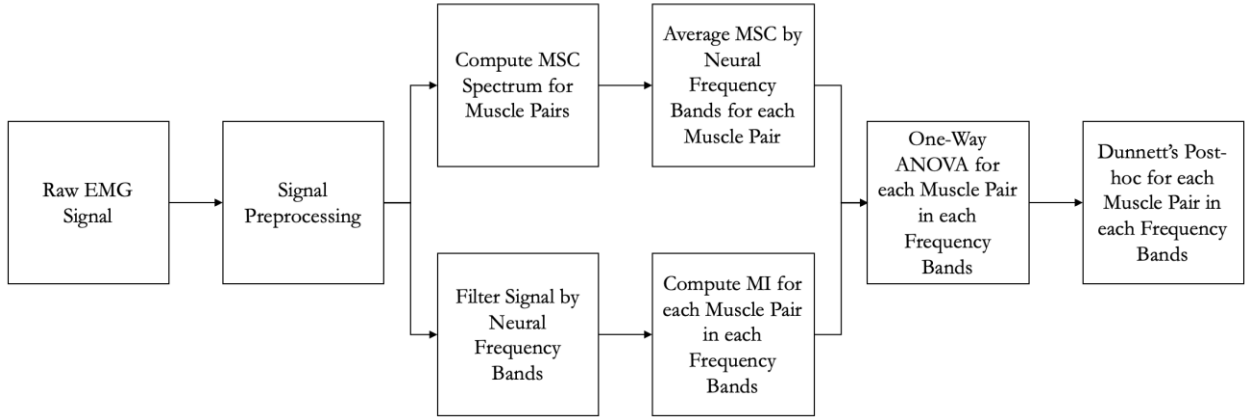


Figure 2.1: Functional block diagram of the data analysis process

2.2.4.1. Signal Preprocessing

MATLAB's Welch's power spectral density (PSD) estimator was used to visually analyze the frequency content of the raw 30-second EMG data collected for baseline condition, for all muscles, and each subject to identify any noise artifacts. A 60 Hz 2nd-order Butterworth notch filter with a 0.2 Hz bandwidth was used to remove the powerline interference at 60 Hz.

2.2.4.2. Magnitude Squared Coherence

Magnitude squared coherence (MSC) measures the linearity of the phase relation between two signals x and y in the frequency domain defined by

$$C_{xy} = \frac{|S_{xy}(f)|^2}{S_{xx}(f)S_{yy}(f)} \quad (2.1)$$

C_{xy} is MSC, S_{xy} is the cross-spectrum power and S_{xx} and S_{yy} are the auto-spectrums of input signals x and y at frequency f . MSC values are evaluated between 0 and 1, where 0 indicates no linear relationship and 1 is a perfect linear relationship. The use of intermuscular, EMG-EMG, coherence provides insight into the connectivity between EMG signals of neighboring leg muscles.

MSC was calculated from MATLAB's built in MSC function that estimates C_{xy} using Welch's overlapped periodogram method. The MSC spectrum was estimated for the whole 30-seconds of all filtered EMG data for each muscle pair listed in Table 2.1 across the neural frequency range (0 – 100 Hz) for each standing condition, and each subject. MSC was estimated from two-second Hamming window, with 25% overlap. This created 19 window segments of 2400 data points and a frequency resolution of 0.5 Hz. Each neural frequency range was averaged across its MSC spectrum to generate a singular coherence value for that range.

2.2.4.3. Mutual Information

Mutual information (MI) is an information theoretic measurement that measures the information dependence between two random variables defined as

$$I(X, Y) = \sum_x \sum_y p(x, y) \log_2 \frac{p(x, y)}{p(x)p(y)} \quad (2.2)$$

$I(X, Y)$ is MI, $p(x, y)$ is the joint probability distribution and $p(x)p(y)$ is the product probability distribution of input signals x and y . MI is based on the fundamental concept of entropy that was introduced by Shannon [30]. MI defined by its entropic, degree of uncertainty, properties is shown as

$$I(X, Y) = H(X) + H(Y) - H(X, Y) \quad (2.3)$$

Where $H(X)$ and $H(Y)$ are individual entropies, and $H(X, Y)$ is the joint entropy defined as

$$H(X) = - \sum_{i=1}^n p(x_i) \log_2 p(x_i) \quad (2.4)$$

$$H(X, Y) = - \sum_x \sum_y p(x, y) \log_2 p(x, y) \quad (2.5)$$

Joint and individual entropy is the degree of uncertainty based on joint probability distribution $p(x, y)$ and individual probability mass function $p(x_i)$ respectively. MI quantifies that future values of X can be better predicted from also knowing past values of Y . MI is the reduction of uncertainty of knowing X given Y .

MI was obtained using the MIDER toolbox for MATLAB created by Villanverde et al. [29]. The normalization method that was employed was created by Michaels et al. [31] in the context of analyzing large-scale gene expression defined as

$$I_{NM}(X, Y) = \frac{I(X, Y)}{\max(H(X), H(Y))} \quad (2.6)$$

Normalized MI allows for the comparison of MI with other calculated MI values in the 0 to 1 range based off of the maximal entropy of each contributing time series [31].

MI was calculated between the same 9 muscle pairs, that were shown in Table 2.3, MSC was. In order to make MI comparable to MSC EMG data sets were manipulated similar to how MSC was calculated. 4th order Butterworth lowpass and bandpass filters were applied to the EMG signals to view only the signals present in each of the neural frequency bands of interest as listed in Table 2.2. MIDER was implemented over 2400 data point segments with 25% overlap to create 19 segments

for MI. The average MI of the 19 segments was used for each muscle pair, frequency band, standing condition, and subject.

2.2.4.4. *Statistical Analysis*

For each subject individual one-way ANOVAs were analyzed for each muscle pair in each frequency band of interest for MSC and MI. Each subject was considered independent of one another regardless of their foot dominance based on the assumption that each subject has a postural control system unique to them. One-way ANOVA was used to compare the mean coherence between each standing task within each subject for each muscle pair and frequency band. Each trial was assumed to be independent of subsequent trials within each condition. In this sense it is assumed that trial 1 and trial 5 are independent of each other. Dunnett's post-hoc two-sided t-test was used to examine which coherence frequency bands of the less stable conditions differed from the baseline condition. This analysis was then repeated for MI.

2.3. Results

2.3.1. Magnitude Squared Coherence

Each subject was observed to be independent of each other. All 9 muscles pairs were compared across standing condition and the neural frequency range of interest. MSC spectrum for each muscle pair was averaged over the neural frequency band ranges for each subject. This is shown in Figure 2.2 - Figure 2.7. The results of the individual one-way ANOVAs, for each subject, is indicated with *significance at $p < 0.05$, **significance at $p < 0.01$, and ***significance at $p < 0.001$. Subjects, denoted with "SB", and their foot dominance was known for between subject comparisons. Subjects 1 – 3 were right foot dominant (RFD) and subjects 4 – 6 were left foot dominant (LFD).

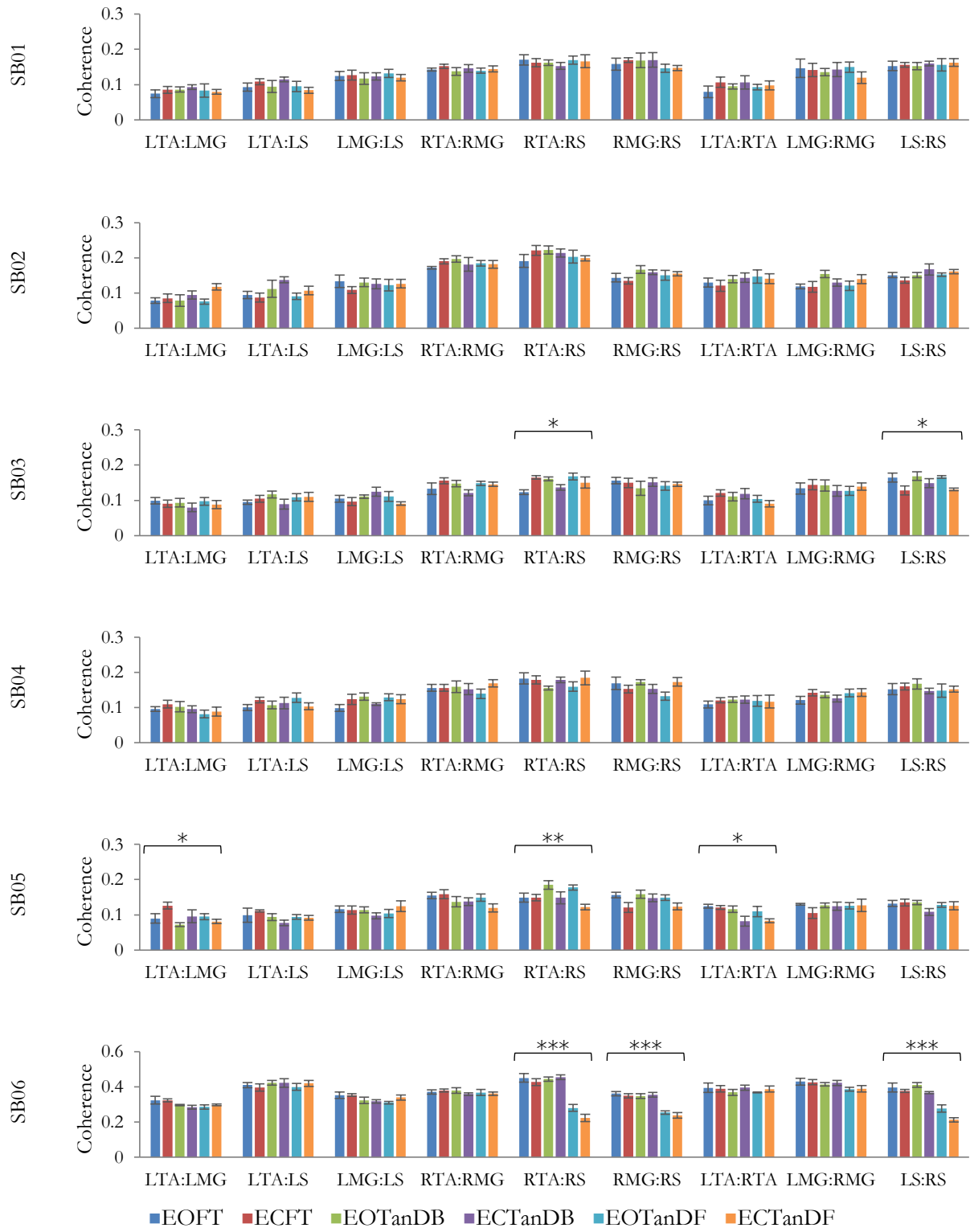


Figure 2.2: Average and standard error of the mean MSC in the delta band

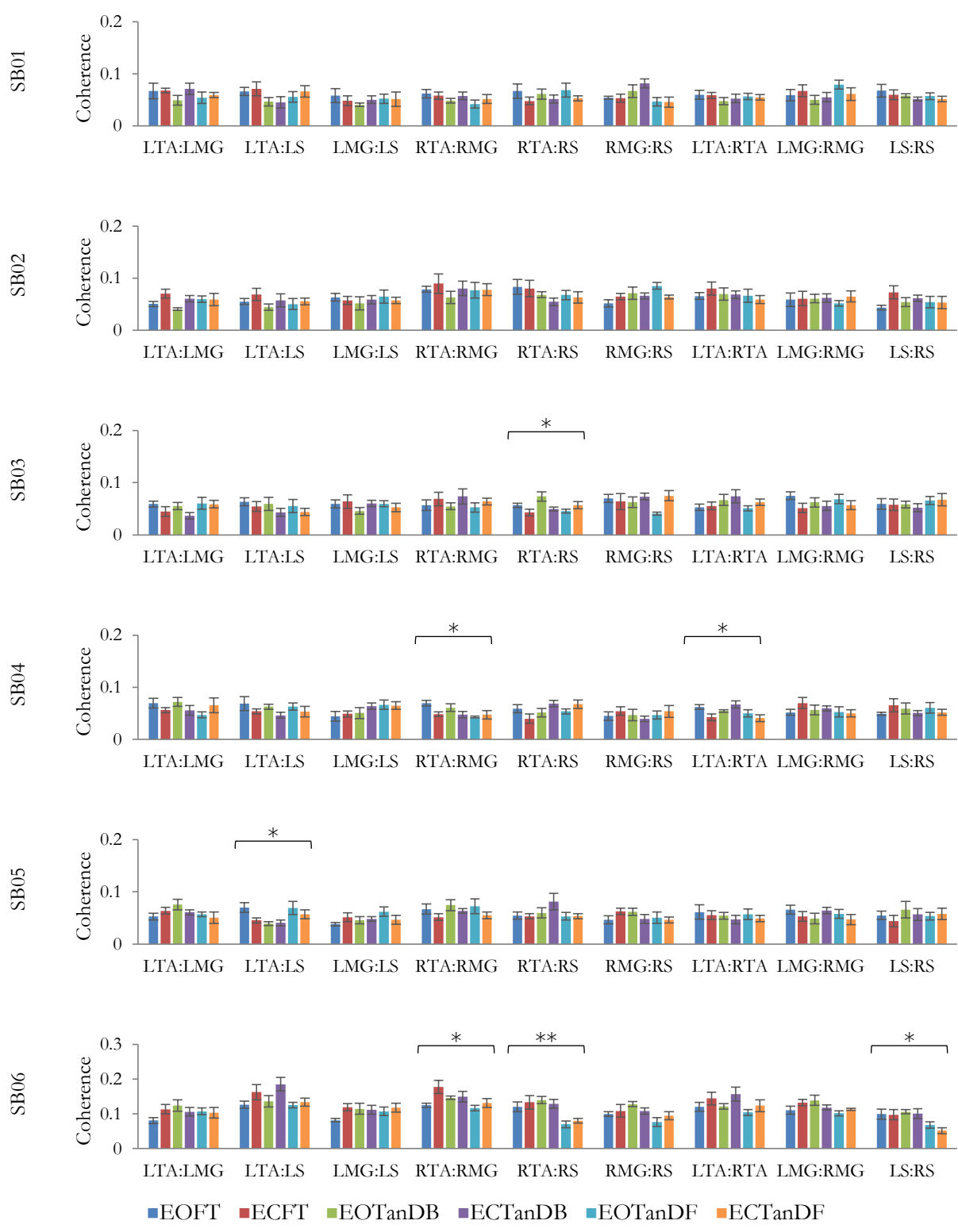


Figure 2.3: Average and standard error of the mean MSC in the theta band

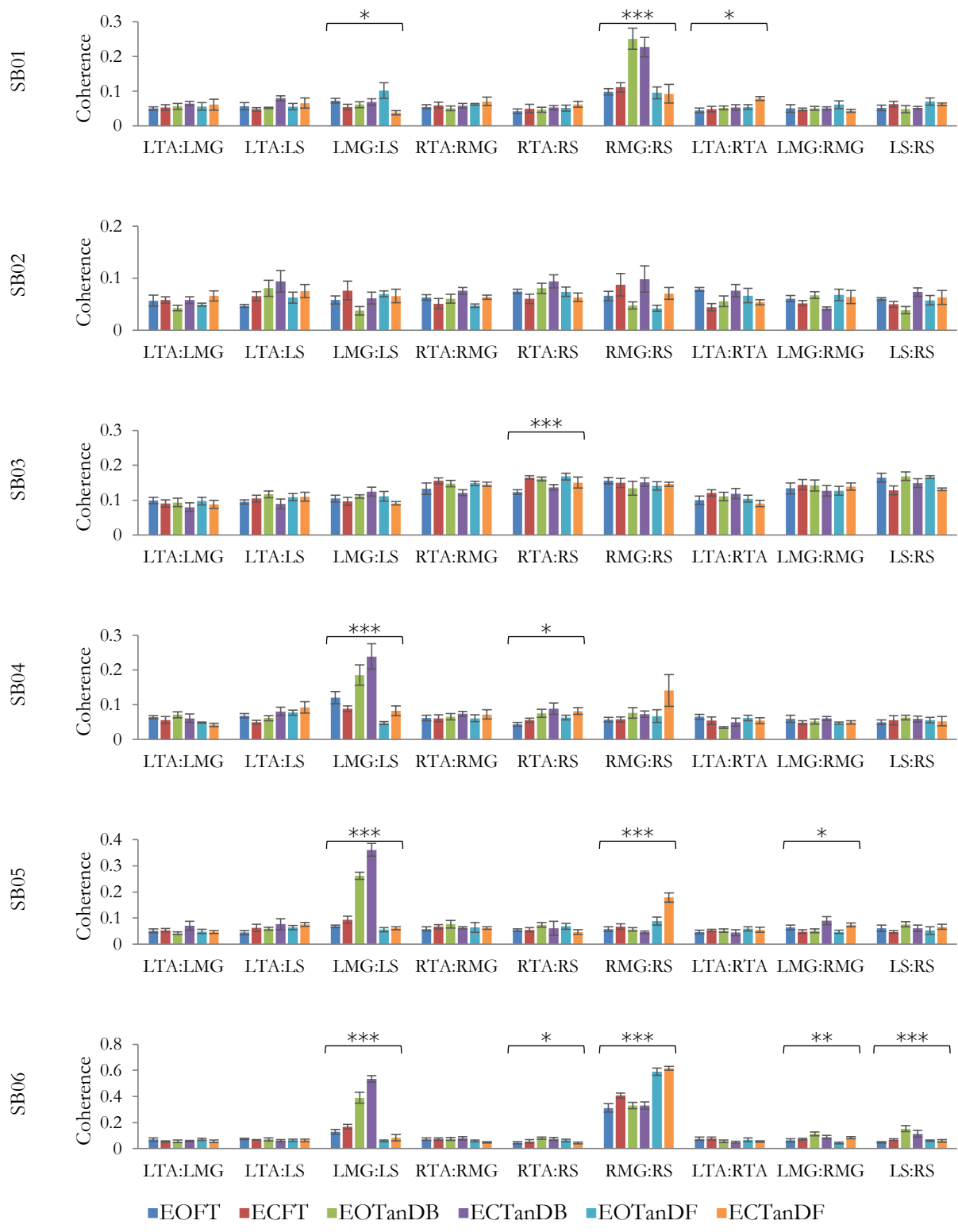


Figure 2.4: Average and standard error of the mean MSC in the alpha band

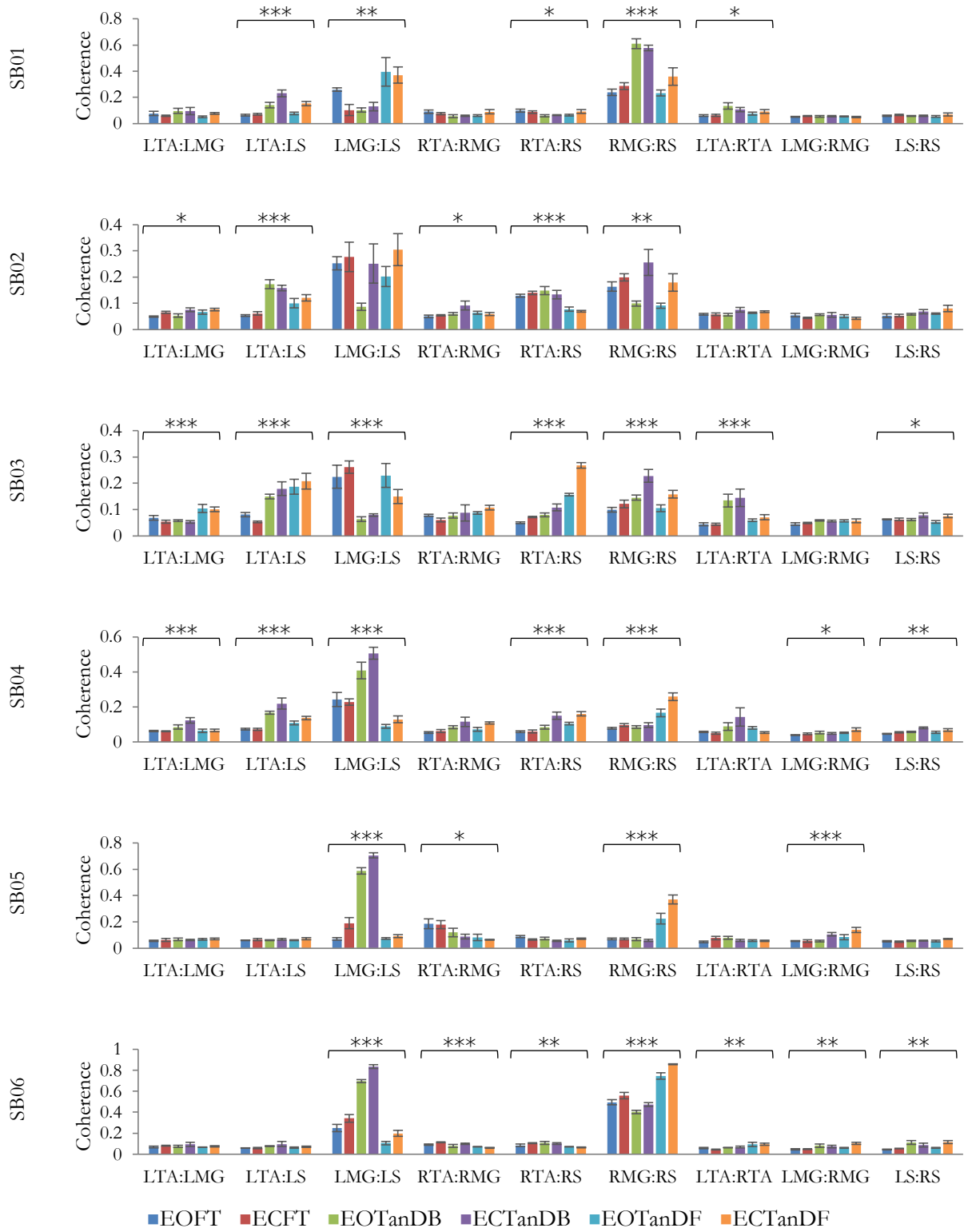


Figure 2.5: Average and standard error of the mean MSC in the beta band

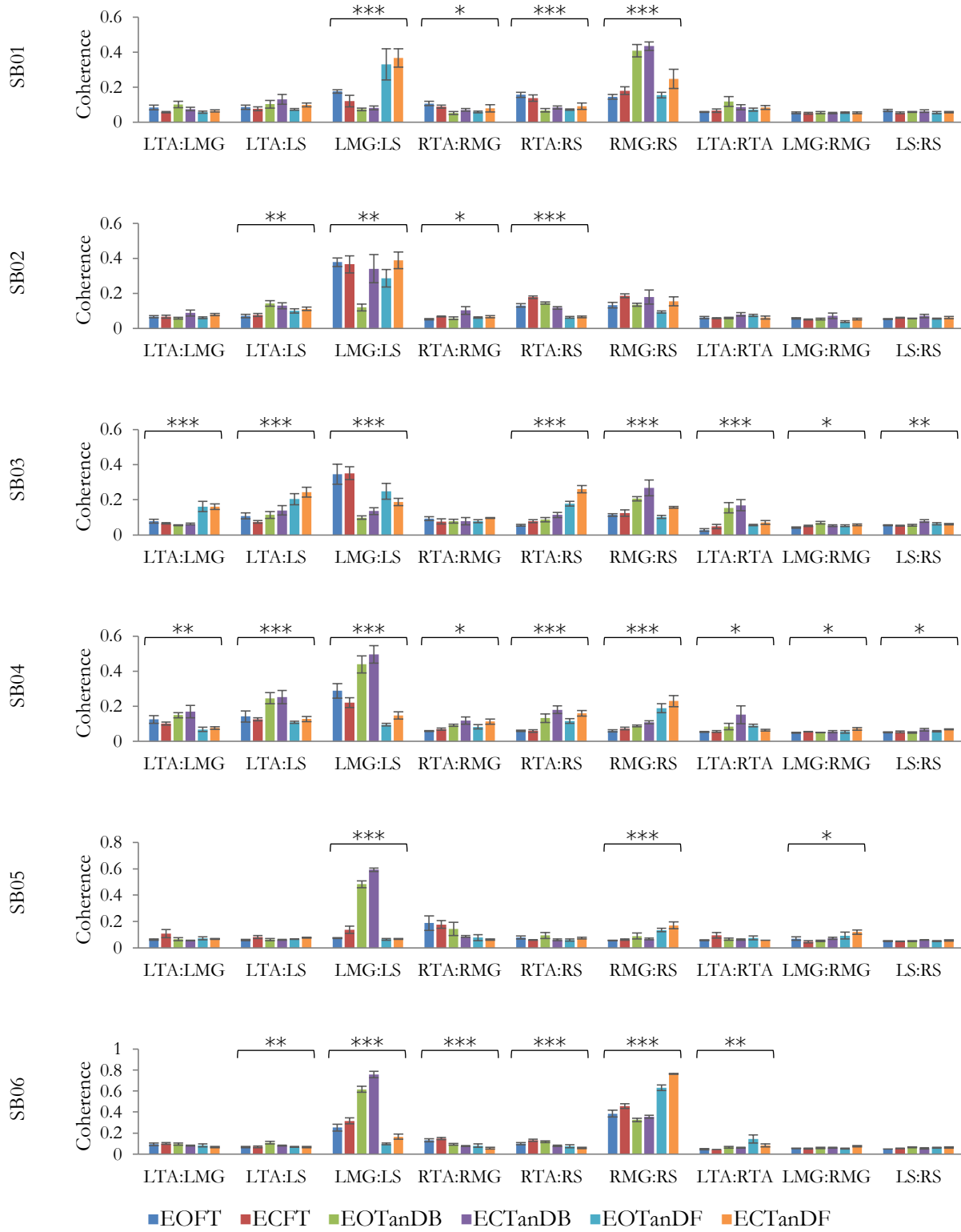


Figure 2.6: Average and standard error of the mean MSC in the lower gamma band

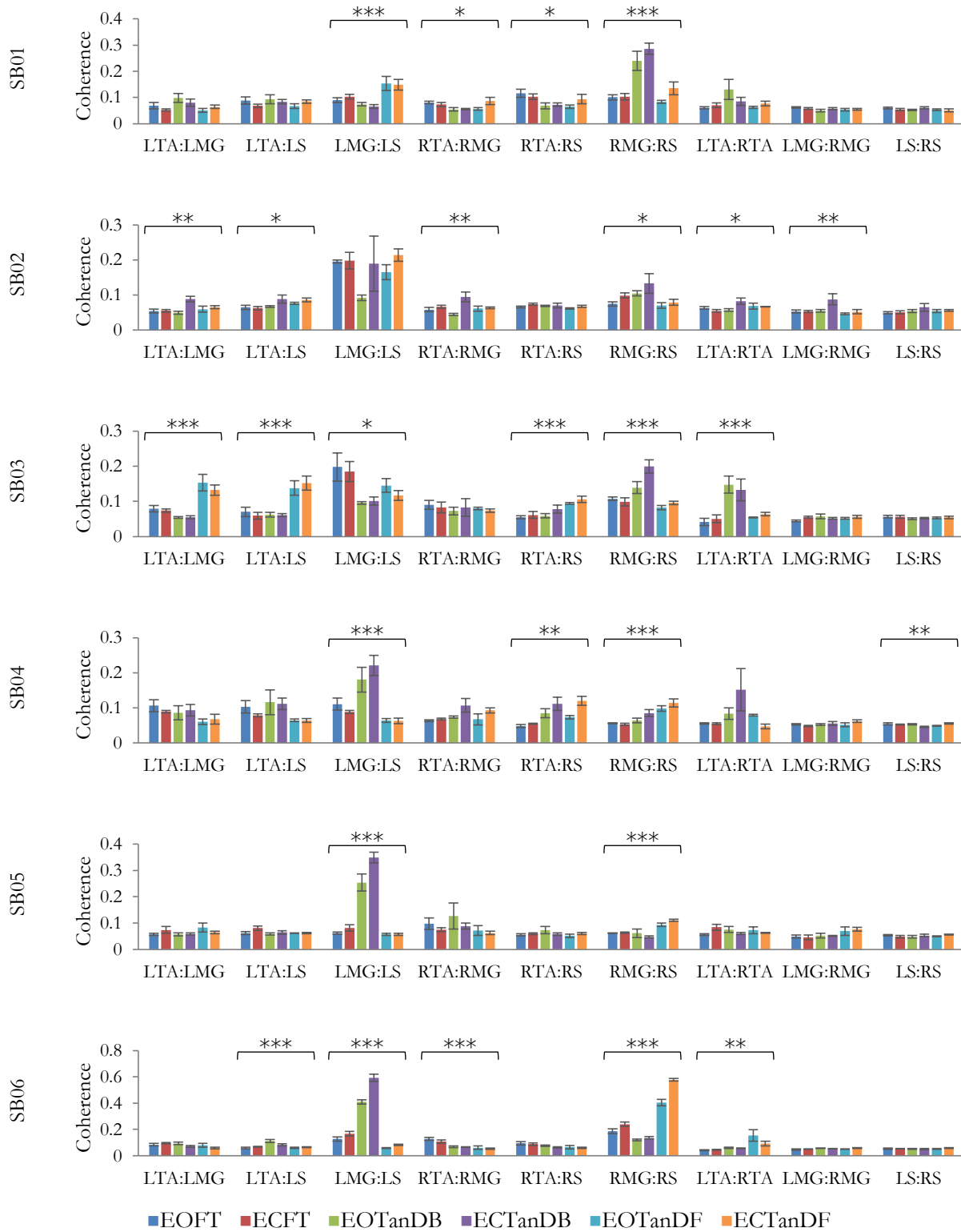


Figure 2.7: Average and standard error of the mean MSC in the upper gamma band

From Figure 2.2 the delta band had the largest amplitude in coherence across all muscle pairs and conditions for all subjects. The muscle pairs of the right leg had a slightly larger coherence amplitude than the left muscle pairs and was more noticeable in the RFD subjects. Across the muscle pairs coherence does not appear to significantly change from baseline during various balance conditions. SB06 displayed significantly larger, overall, coherence in the delta band compared to the other subjects.

The theta band, Figure 2.3, coherence showed more variability than delta band between standing task conditions. Distribution appears to be uniform across muscle pairs for each subject and condition. Only a few subject's muscle pairs had significance in the theta band. SB06 displayed significantly larger, overall, coherence in the theta band compared to the other subjects.

The alpha band, Figure 2.4, shows a distinct coherence pattern emerging in the LMG:LS muscle pair of LFD subjects when in TanDB stance.

The beta band, Figure 2.5, carries the same distinct coherence pattern that emerged in the alpha band for the LMG:LS muscle pair for LFD subjects. Additional significance is also observed in the RMG:RS muscle of the LFD subjects. RFD subjects showed significance in the LMG:LS and the RMG:RS similar to LFD subjects. Additional significance was found in the RTA:RS and LTA:LS for RFD subjects. The amount of significant muscle pairs increased from alpha to beta band.

Lower gamma band coherence, shown in Figure 2.6, showed significance in the LMG:LS in all subjects. All subjects except SB02 showed significance in the RMG:RS muscle pair. SB03 and SB04 had the highest occurrence of significance across the muscle pairs.

The upper gamma band (Figure 2.7) showed significant coherence in the RMG:RS muscle pair across all subjects. All subjects except SB02 showed significance in the LMG:LS muscle pair. The amount of significant muscle pairs decreased from lower gamma to upper gamma band.

Dunnett's 2-sided post-hoc t-test was performed for all muscle pairs that were found to be significant in each neural frequency band for each subject by the one-way ANOVA. The majority of the muscle pairs, for each subject between the standing task conditions, did not show significance in the delta, theta, or alpha bands. The post -hoc results for these bands are found in Appendix A. The post-hoc results for alpha, beta, lower gamma, and upper gamma are shown in Figure 2.8 - Figure 2.11.

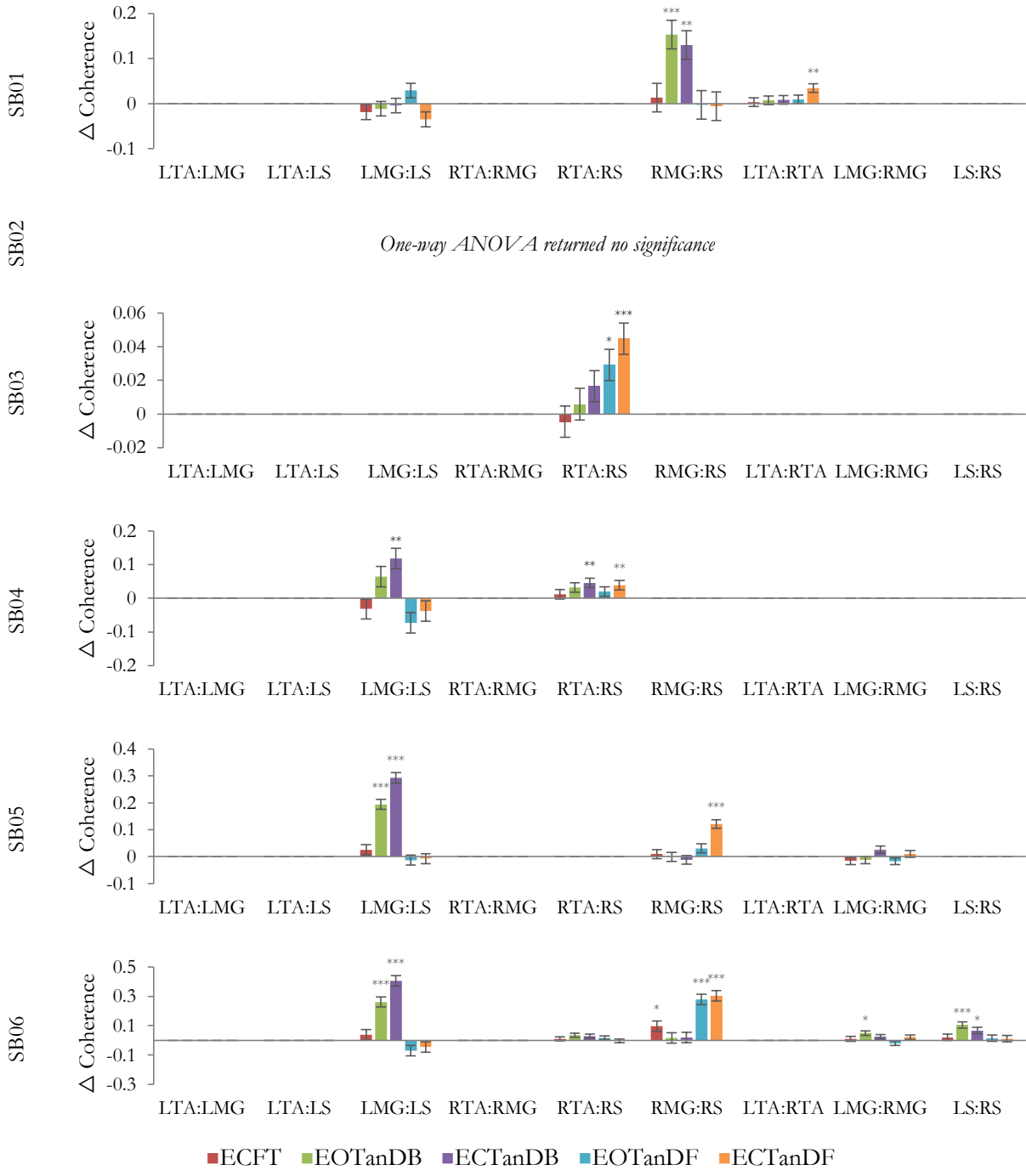


Figure 2.8: Results of Dunnett's two-sided post-hoc t-test for multiple comparisons against baseline (EOFT) condition for significant MSC in the alpha band

Post-hoc results for the alpha band, shown in Figure 2.8 showed that the LFD subjects showed the greatest change in coherence from baseline in the ECTanDB condition in the LMG:LS muscle pair.

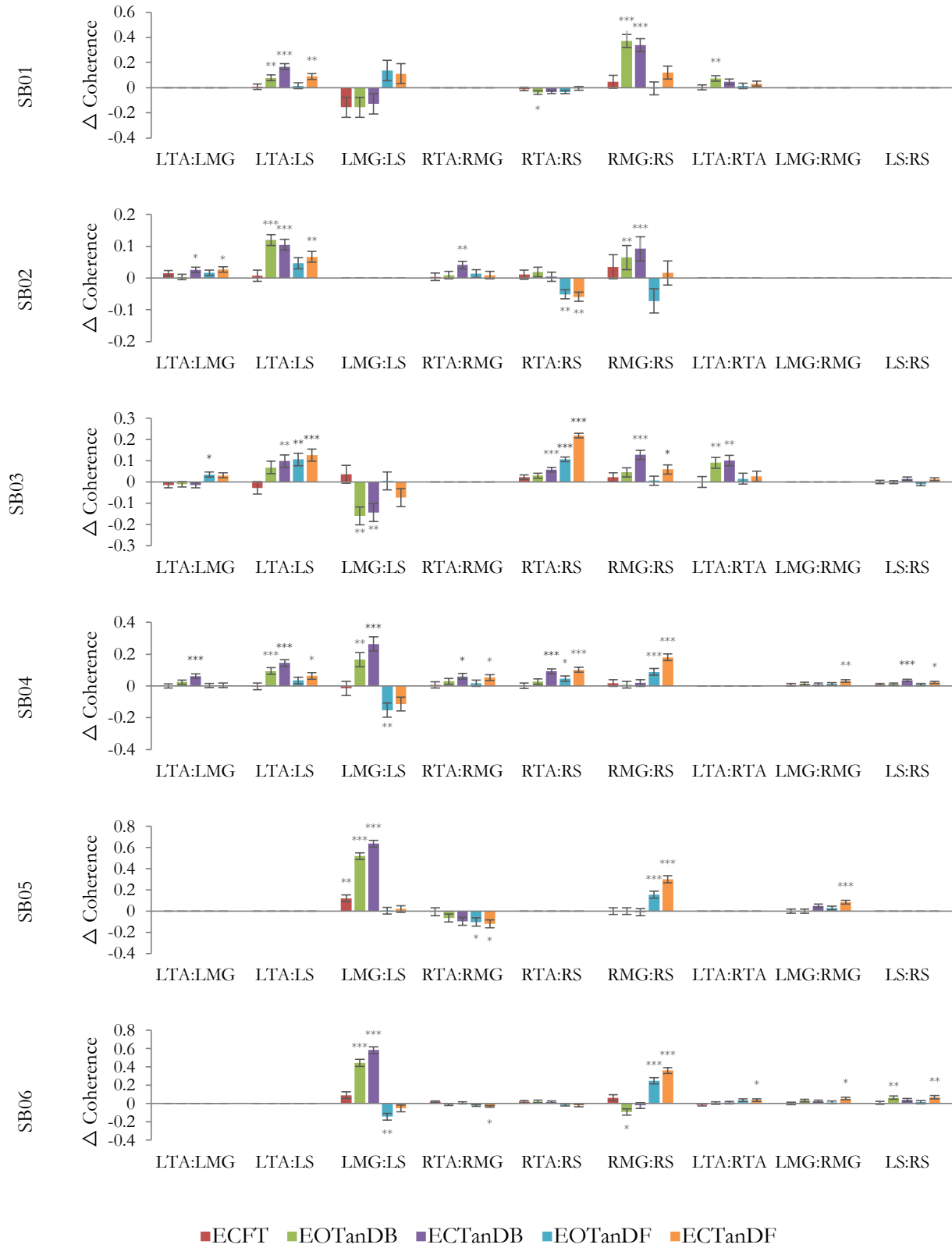


Figure 2.9: Results of Dunnett's two-sided post-hoc t-test for multiple comparisons against baseline (EOFT) condition for significant MSC in the beta band

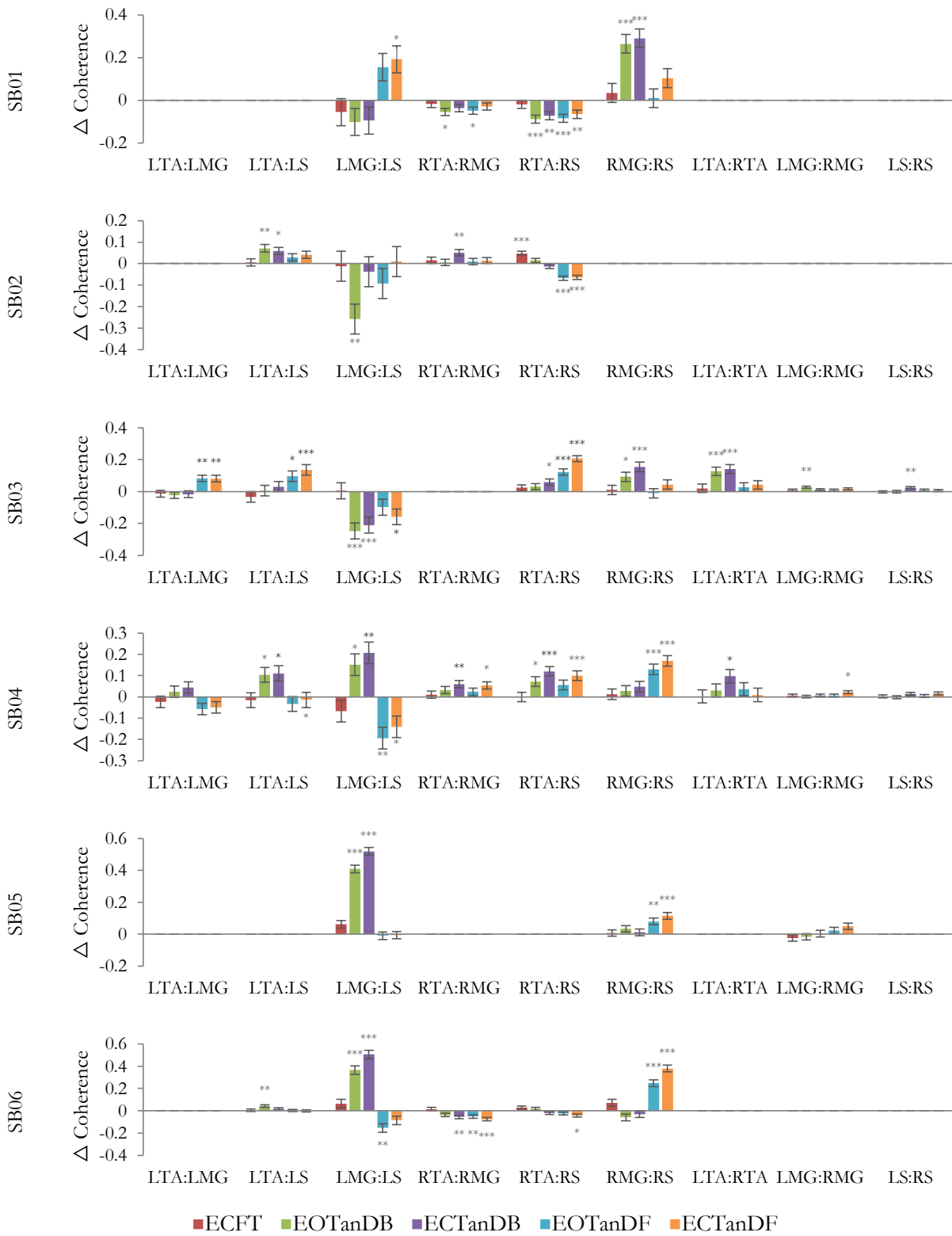


Figure 2.10: Results of Dunnett's two-sided *post-hoc t*-test for multiple comparisons against baseline (EOFT) condition for significant MSC in the lower gamma band

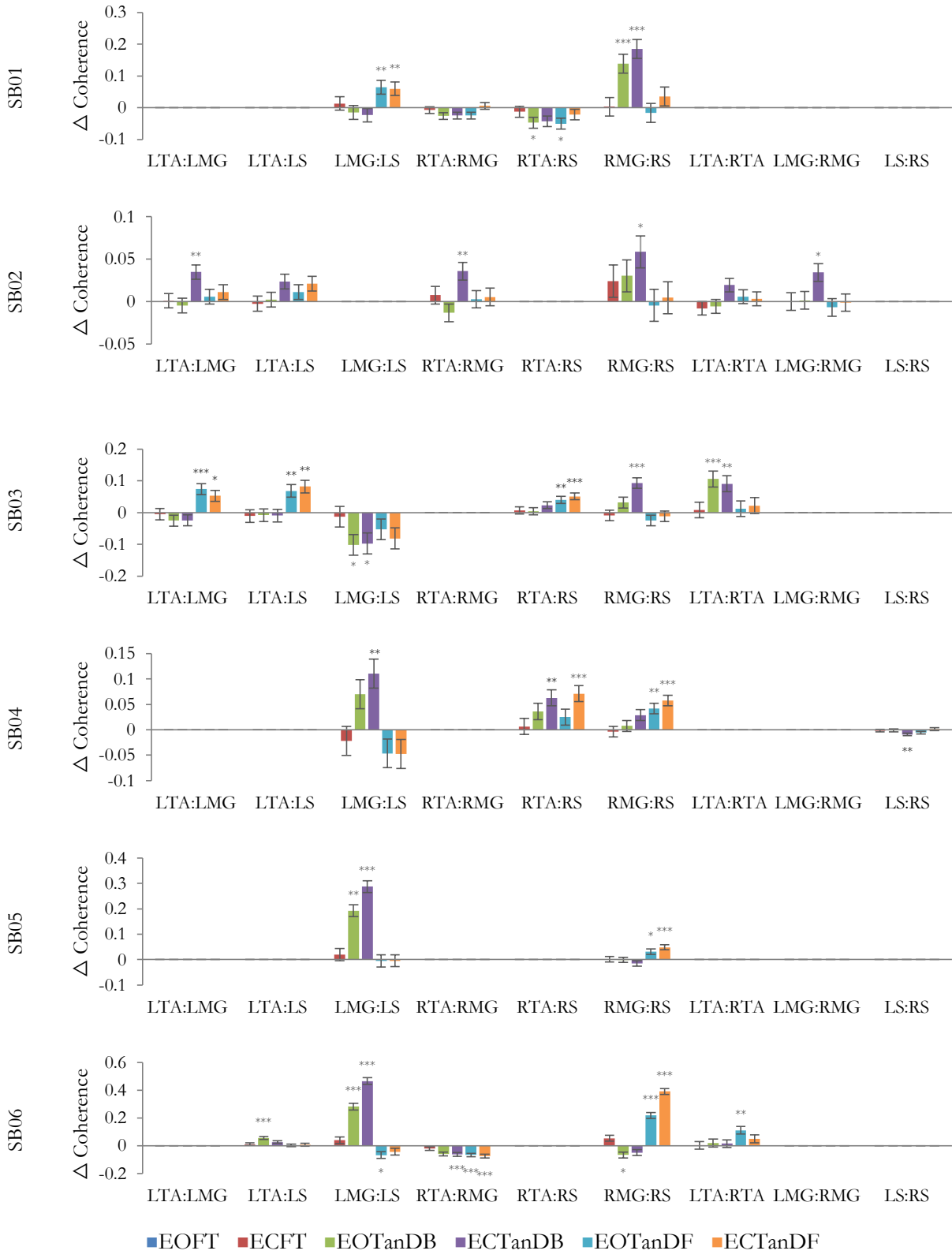


Figure 2.11: Results of Dunnett's two-sided post-hoc t-test for multiple comparisons against baseline (EOFT) condition for significant MSC in the upper gamma band

The beta band post-hoc results demonstrated that both TanDB stances showed significance in the LMG:LS muscle pair of LFD subjects this is shown in Figure 2.9. Coherence increased from baseline in TanDB stance. EC had a larger change in coherence than EO in TanDB from baseline. Additional significance was observed in the TanDF stance for RMG:RS with increased coherence and EC having greater coherence than EO. For RFD subjects significance is seen in the LTA:LS across all tandem stances for increased coherence from baseline. The RMG:RS muscle pair showed significance in increased coherence from baseline to TanDB stances.

The lower gamma band post-hoc showed significance in the LMG:LS in TanDB stance of LFD subjects and in TanDF of RFD subjects this is shown in Figure 2.10. In the RMG:RS muscle pair LFD subjects showed significance in TanDF and RFD subjects in the TanDB. The LFD subjects demonstrated a decrease in coherence in LMG:LS during TanDF.

The upper gamma band, Figure 2.11, showed significant coherence similar to the lower gamma band where LFD subjects had increased coherence during TanDB in the LMG:LS pair and RFD during TanDF in the RMG:RS pair. LFD subjects showed a larger change in coherence for EC than EO of TanDB for LMG:LS. The RMG:RS pair, of LFD, also had a larger increase coherence for EC than EO of TanDF. RFD subjects showed greater change in coherence in the TanDB for EC and EO in the RMG:RS muscle pair.

2.3.2. Mutual Information

The results of the individual one-way ANOVAs for averaged MI, for each muscle pair, across each frequency band, and for each subject is shown in Figure 2.12 - Figure 2.17 with *significance at $p < 0.05$, **significance at $p < 0.01$, and ***significance at $p < 0.001$.

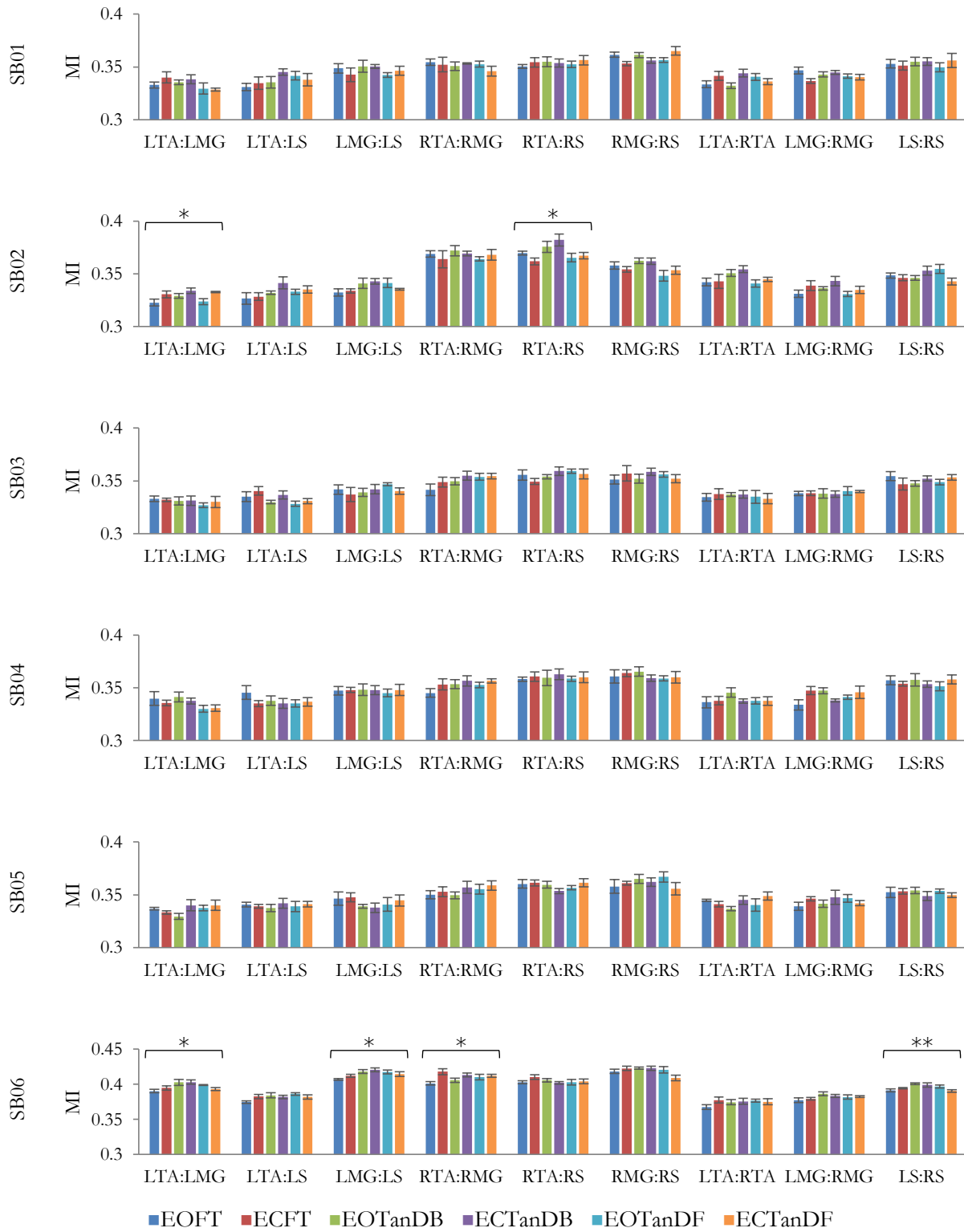


Figure 2.12: Average and standard error of the mean MI in the delta band

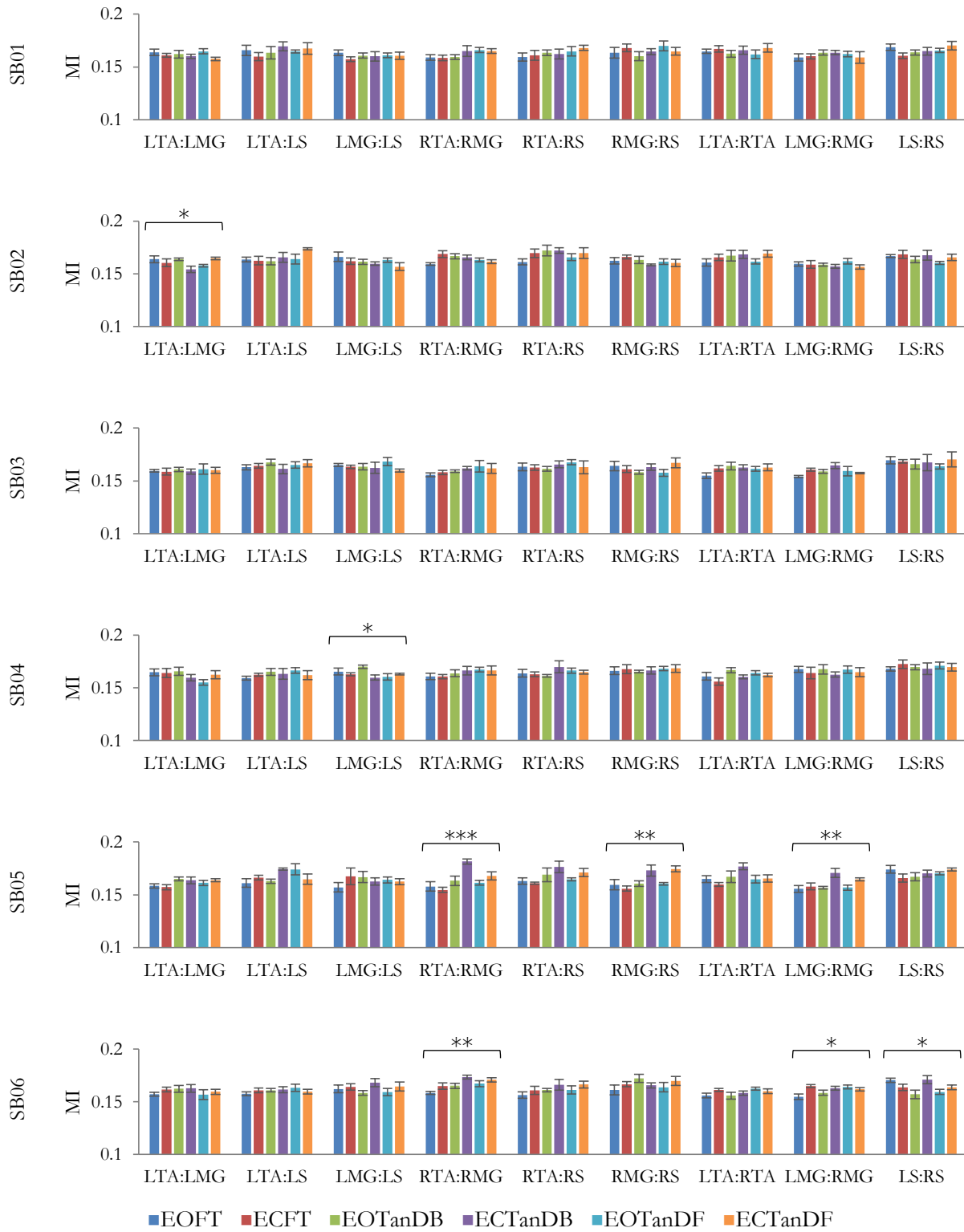


Figure 2.13: Average and standard error of the mean MI in the theta band

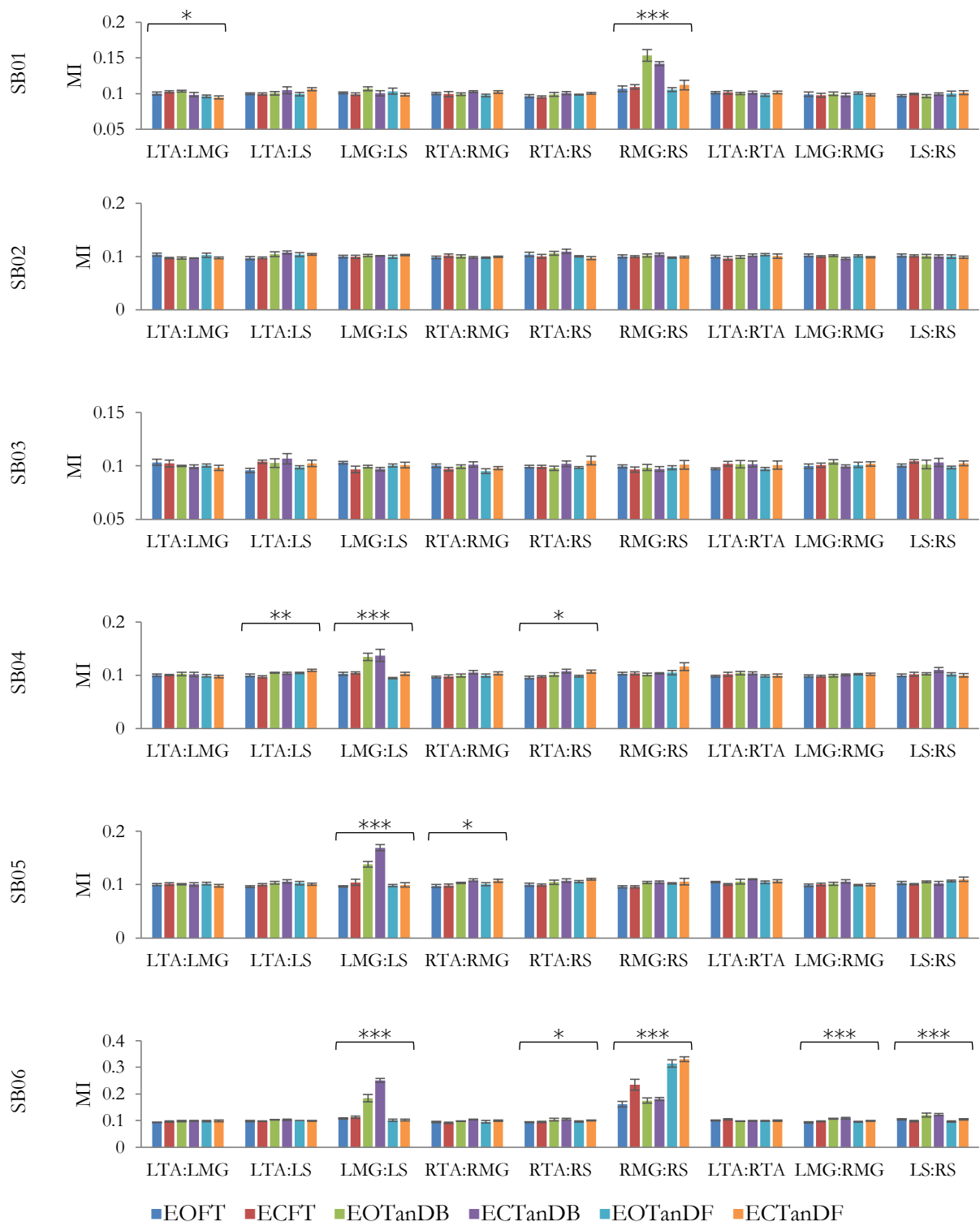


Figure 2.14: Average and standard error of the mean MI in the alpha band

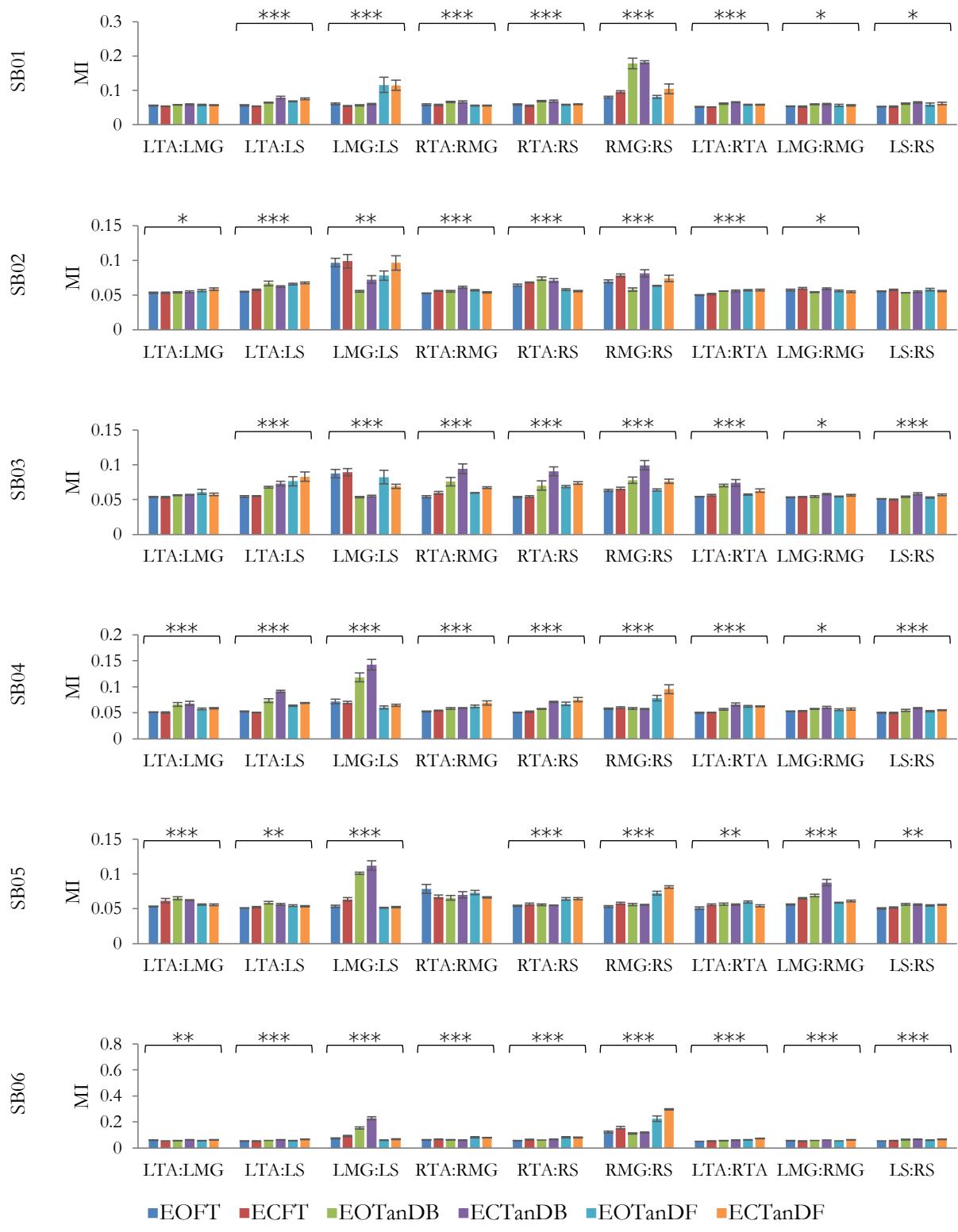


Figure 2.15: Average and standard error of the mean MI in the beta band

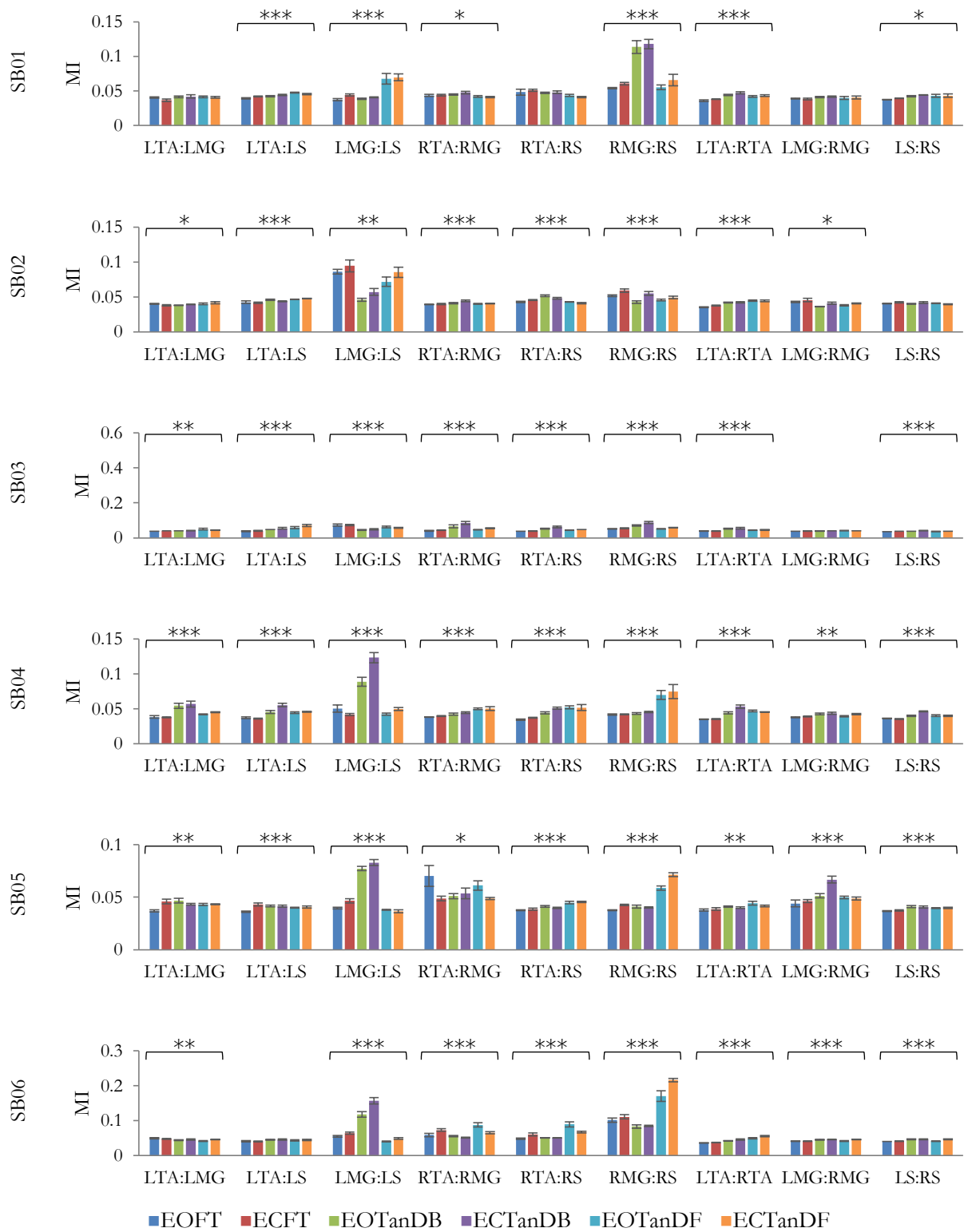


Figure 2.16: Average and standard error of the mean MI in the lower gamma band

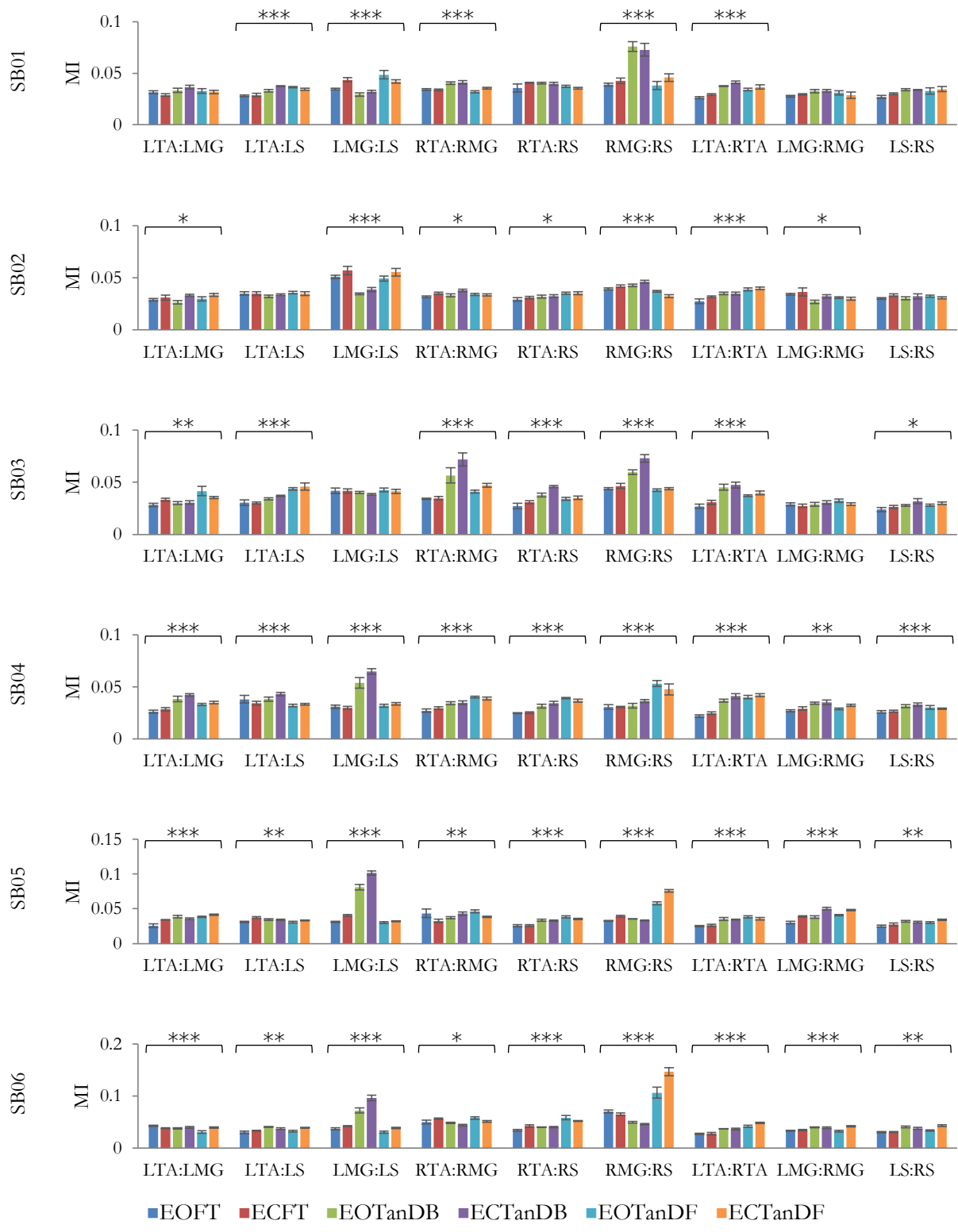


Figure 2.17: Average and standard error of the mean MI in the upper gamma band

The delta band, Figure 2.12, had the greatest amplitude of MI. Right unilateral muscle pairs had a noticeably larger amplitude of MI compared to left unilateral and bilateral homologous muscle pairs. Overall MI for each muscle pair across standing task conditions showed no significant change. Only SB02 and SB06 had some significance in a few pairs.

Overall MI for theta band, Figure 2.13, showed no distinct patterns across muscle pairs or conditions. Only a few subjects showed significance in a few muscle pairs.

MI for alpha band, Figure 2.14, found significance in the LMG:LS muscle pair for LFD subjects. Distinctions are more noticeable between standing conditions compared to delta and theta bands for some subjects. SB02 and SB03 showed no significance in this band.

MI for the beta band, Figure 2.15, lower gamma band, Figure 2.16, and upper gamma band, Figure 2.17, found significance across almost all muscle pairs for all subjects. Results from Dunnett's 2-sided post-hoc t test will give more insight in the significance found. The LMG:LS muscle pair for SB02 in the lower gamma band appears to be significant but its $p = 0.063$.

Dunnett's 2-sided post-hoc t-test was used on all muscle pairs that were found to be significant in each neural frequency band for each subject. The majority of the muscle pairs, for each subject between standing task conditions, did not show significance in the delta, theta, or alpha bands. The post-hoc results for the delta and theta bands are found in Appendix A. The post-hoc results for alpha, beta, lower gamma, and upper gamma are shown in Figure 2.18 - Figure 2.21.

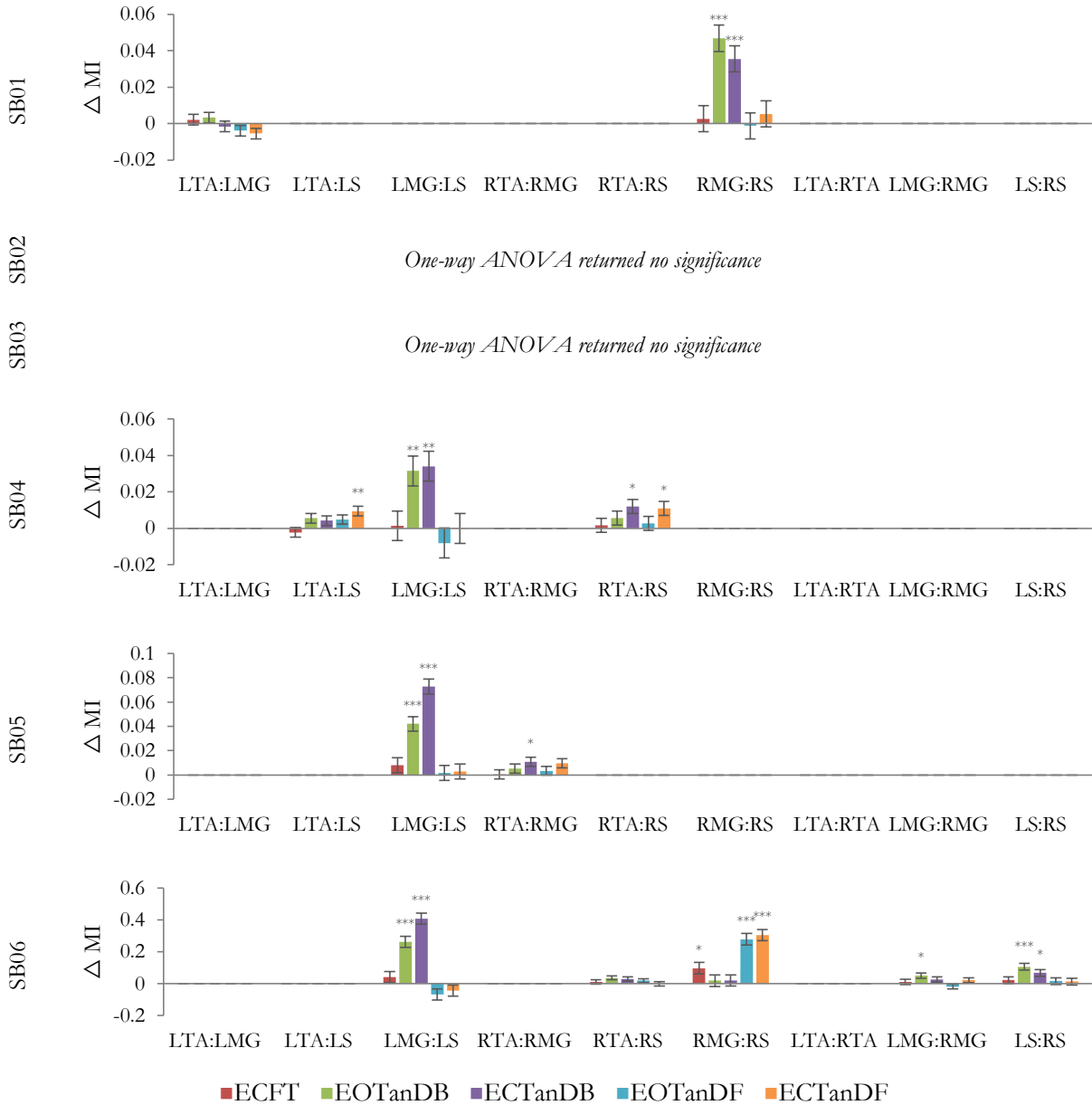


Figure 2.18: Results of Dunnett's two-sided post-hoc t-test for multiple comparisons against baseline (EOFT) condition for significant MI in the alpha band

The alpha band only shows discernable significance for LFD subjects. Across all LFD subjects the LMG:LS muscle pair showed significance and increased MI from baseline condition during TanDB stance. EC showed a greater change in MI than EO when compared to baseline.

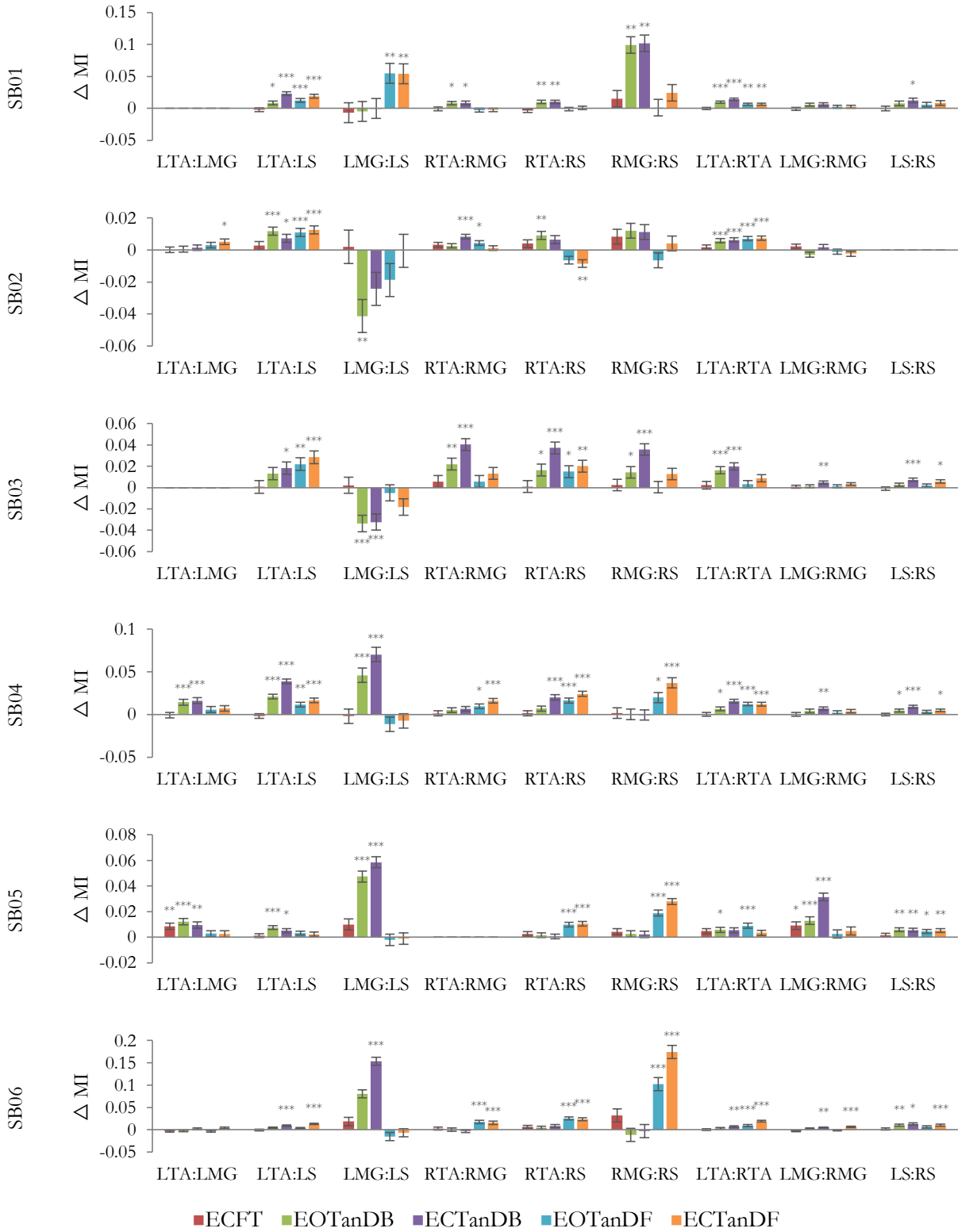


Figure 2.19: Results of Dunnett's two-sided post-hoc t-test for multiple comparisons against baseline (EOFT) condition for significant MI in the beta band

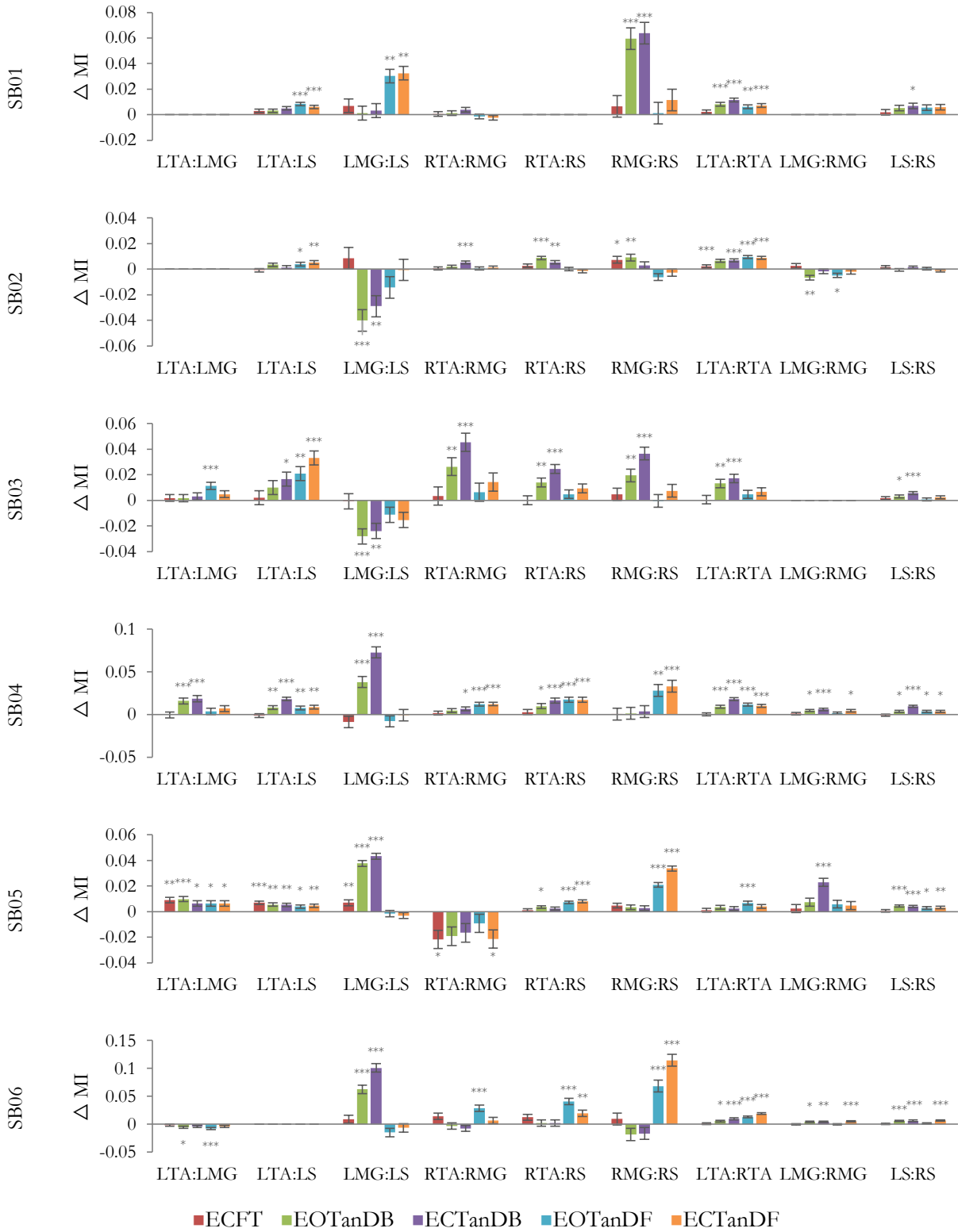


Figure 2.20: Results of Dunnett's two-sided post-hoc t-test for multiple comparisons against baseline (EOFT) condition for significant MI in the lower gamma band

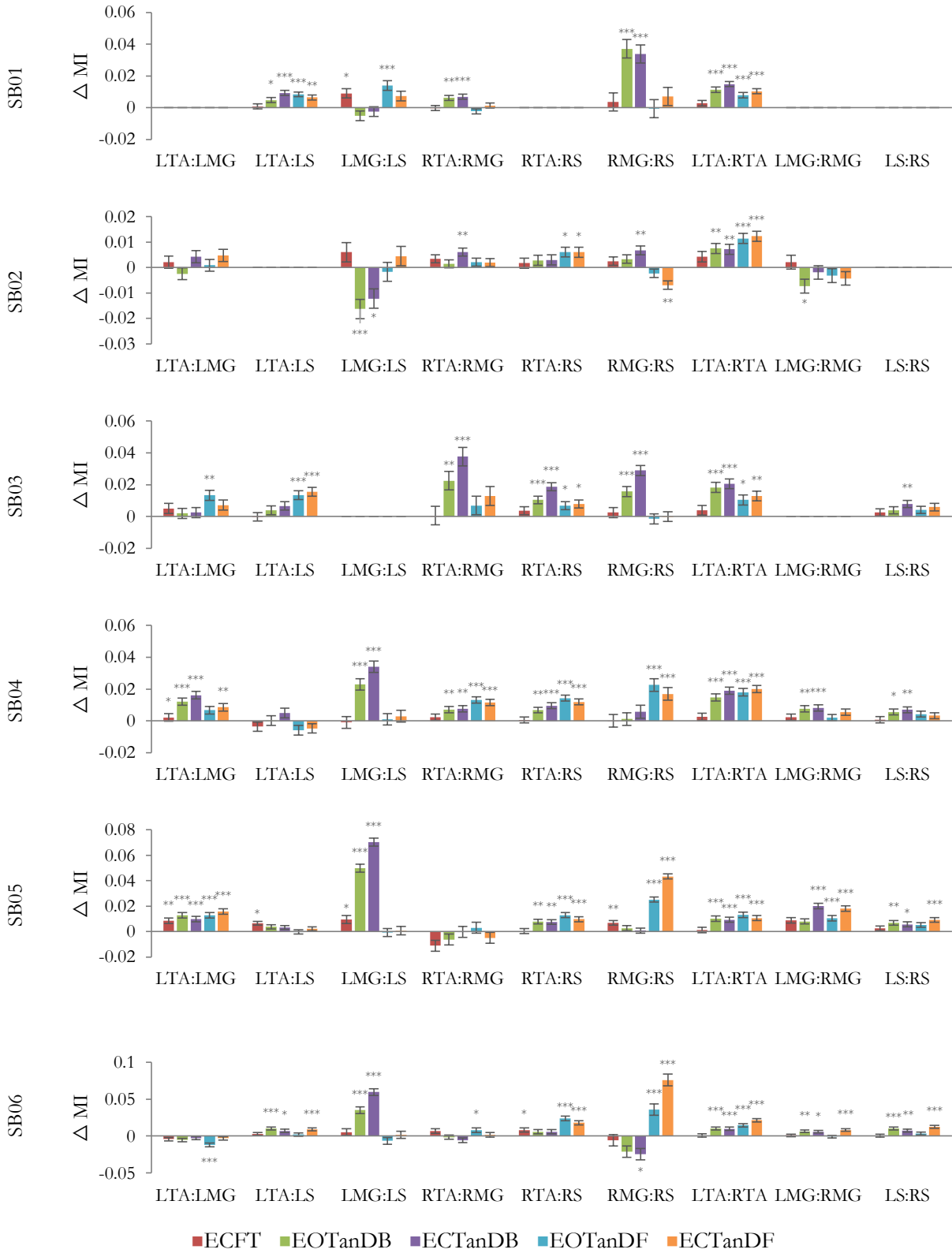


Figure 2.21: Results of Dunnett's two-sided post-hoc t-test for multiple comparisons against baseline (EOFT) condition for significant MI in the upper gamma band

In the beta band, Figure 2.19, all RFD subjects showed significance in all muscle pairs except LTA:LMG and LS:RS. ECFT showed no significance in any of the muscle pairs. The RMG:RS pair increased MI during TanDB stance. The LFD subjects showed increased MI in the LMG:LS muscle pair during TanDB and in the RMG:RS muscle pair during TanDF stance. EC had greater change in MI than EO in these pairs during these stances. All subjects showed significance and increased MI in the LTA:RTA and the LTA:LS muscle pairs across all conditions. All subjects except SB02 showed significance and increased MI in the LS:RS muscle pair. Overall the right unilateral muscle pairs of RFD subjects showed significance in the TanDB stance. For LFD subjects the left unilateral muscle pairs showed significance in the TanDB while the right unilateral muscle pairs showed significance in the TanDF stance. All bilateral homologous muscle pairs showed significance for LFD subjects.

In the lower gamma band, Figure 2.20, RFD subjects showed significant MI in the RMG:RS muscle pair during TanDB stance. LFD subjects showed significant MI in the LMG:LS during TanDB stance and in the RMG:RS muscle pair during TanDF stance. Between EC and EO, EC showed more change in MI than EO. All subjects showed coherence in the LTA:RTA muscle pair. Overall the right unilateral muscle pairs of RFD subjects showed significance in the TanDB stance. For LFD subjects and the left unilateral muscle pairs showed significance in the TanDB while the right unilateral muscle pairs showed significance in the TanDF stance.

The upper gamma band, Figure 2.21, showed similar results of the lower gamma band. The LFD subjects showed significant increased MI in all the bilateral homologous muscle pairs. Similar to the lower gamma and beta bands the left unilateral muscle pairs showed significance in the TanDB while the right unilateral muscle pairs showed significance in the TanDF stance for LFD subjects. All bilateral homologous muscle pairs showed significance for LFD subjects.

2.4. Discussion

In order for humans to maintain balance a continuously active postural control system is implemented by the CNS. The use of MSC and MI analysis methods showed the existence of similar patterns that could be indicative of neural connectivity. In this study the role of foot dominance as well as each subject's individual postural control system was evaluated. It was assumed that postural control differed between individuals simply due to each individual's characteristics of lifestyle, present activity level, and activity history. However, the possible use of a common neural drive implemented by the CNS to control postural control muscles may stretch across all subjects. Thus, subjects may share similar activations or coherence due to a similar postural task. This response helps to quantify how the CNS is able to operate the musculoskeletal system.

2.4.1. Connectivity

2.4.1.1. *Neural Connectivity*

Both MSC and MI showed that delta band had the largest amplitude of both coherence and MI among all conditions and subjects. Between conditions the delta band did not show any change in either coherence and MI. Studies have shown that high coherence in the delta band is indicative of postural control [8], [13], [19]. However, the neural origin of this frequency oscillation has yet to be discovered. The theta band did not change significantly between muscle pairs or between standing conditions. Both MSC and MI showed little to no change in the theta band. The amplitude of theta band coherence across the muscle pairs was also constant. In this study theta band coherence and MI was not indicative of any changes in standing tasks in subjects this was shown in the one-way ANOVAs. The overall function of the theta band in quiet standing does not appear to be significant. Studies have found that alpha band showed significant changes when the visual field was altered [10], [15]. In this study neither coherence nor MI was able to find significant enough

changes to frequency content when subjects were asked to close their eyes. This may indicate that alterations to the visual field must be greater than just simply closing of the eyes. Both the beta and lower gamma bands are known to carry signals from the motor cortex [21]. Significance in both the beta and gamma bands occurred when standing task conditions were altered from baseline. This make sense considering the motor cortex is central to moving the musculoskeletal system and may be the reason why significance was observable in both MSC and MI in the beta, lower gamma, and upper gamma bands.

2.4.1.2. *Anatomical Connectivity*

Among the muscle pairs that were analyzed LTA:LMG had low to no connectivity among all subjects and conditions. Bilateral muscle pairs did not show large levels of significance from MSC but MI saw significant connectivity in the beta and gamma bands. Bilateral homologous significance could be indicative of organized neural drive while unilateral significance reflects synergistic muscle coupling [14], [20].

Among all muscle pairs the MG:S pair showed the most significant amount of connectivity similar to a prior study done by Ojha [22]. These muscles are similar in that they are both agonist to each other, part of the same M-mode, and are very close in anatomy. This begs the question if coherence is due to function or rather anatomical location. Some amount of cross-talk may be present in these muscles due to how close in proximity they are to one another. Surface EMGs will no doubt pick up on this cross-talk. Knowing how much of the signal connectivity resulted from cross-talk could give more insight into the actual neural mechanism implemented within these muscles. Further analysis in identifying how these muscles communicate will provide more insight in to the properties of neural control during postural.

2.4.1.3. *Leg Dominance*

Regardless of foot dominance a distinct pattern emerged between connectivity and location of the foot in tandem stance. Connectivity was found to be greatest in the foot that was placed in the back. Rather than favoring their dominant foot during tandem stance it was apparent that regardless of foot dominance coherence was highest in the muscles of the leg that was in the back. If the subsequent standing conditions were not completed by foot dominance it would be difficult to discern foot dominance from either MSC or MI. The sample size in this study was relatively small. The addition of more subjects as well as foot dominance dependent tasks could shed more light in the matter of balance and declared foot dominance. From this study foot dominance does not appear to be a predetermined factor of postural control, rather a learned preference.

2.4.2. **Comparison of Connectivity Analysis Methods**

Both MSC and MI have shown indications of connectivity between the lower leg muscles during various quiet standing conditions. From the change in baseline post-hoc analyses MI showed more overall signal content than MSC. This makes sense considering how MSC is a linear measure of connectivity. EMG is known to have non-linear characteristics. The use of MI was able to pick up these non-linear characteristics and provide more information about the signal content. Both MSC and MI showed that in tandem stance the foot that was placed in the back showed higher signals of connectivity in the muscle pairs in the back leg regardless of declared foot dominance. MI was able to pick up more information about the coupling between antagonistic and bilateral homologous muscle pairs. Unlike MSC, MI compares the content of the signals with each other rather than comparing the signal content to a pre-defined model. The only limitation of MI is computation power. While it may provide better results, and more information, it is time consuming to compare every element of a signal. For one subject MI took close to 30 minutes to calculate.

2.4.3. Limitations and Future Consideration

This study was limited by small sample sizes between RFD and LFD subjects. A larger sample pool would provide more general conclusions about foot dominance as it pertains to postural control. The presence of cross-talk between neighboring muscles was not addressed in the signal analysis. This interaction may have affected to connectivity results of the MG:S muscle pair. Only one pair of agonistic muscles were looked it. In order to verify if connectivity was due to anatomical location or function additional muscles may be beneficial.

Future analyses should look into conditions that involve more distinction in analyzing foot dominance such as stepping or unpredicted perturbations. Order of conditions should not be determined by foot dominance as it may alter the overall comparison of connectivity across subjects when evaluating muscular activation. Increasing the sample size would only benefit this study. The COP data that were collected, and with the full body maker set, could determine COM. Future studies should look at the correlation between COP and COM signals and how they compare with the connectivity results of EMG.

2.5. Conclusion

The use of connectivity analysis provides insight in how the CNS functions to control posture and balance of the multi-segmented musculoskeletal system. There is strong evidence the CNS is able to implement a common neural drive to simultaneously synchronize and activate all the muscles needed to maintain postural stability when balance is disturbed. The delta band shows strong connectivity across various postural tasks, however the beta and lower gamma band showed changes in connectivity during various balance tasks. The underlying neural mechanism of postural control may be dictated by the delta band, but the actual movement may be controlled by the motor cortex. Intermuscular coherence is a popular connectivity analysis method that has been widely used

to assess neural connectivity between muscles. However, by using MI as an information theoretical measurement coherence was found to be lacking in showing connectivity. Both MI and coherence are able to compare agonistic muscle pairs. However, coherence analysis was unable to identifying antagonistic or bilateral homologous connectivity fell short in. Only MI was able to identify significant connectivity between both bilateral homologous and antagonistically paired muscles. The results of this study might change how current studies view the modular organization of the musculoskeletal system and the neural mechanism of postural control.

Chapter 3. Extended Review of Literature and Extended Methodology

3.1. Extended Review of Literature

3.1.1. Motor Control

3.1.1.1. The Central Nervous System

The central nervous system (CNS), consisting of the brain and spinal cord, facilitates the integration of sensory information to coordinate activity throughout the human body. One of the main functions of the CNS is coordinating movement of the musculoskeletal system. The combined process where various sensory inputs dictate certain motor outputs are commonly referred to as sensorimotor processes. The CNS is able to control muscle movement through spinal motor neurons as illustrated in Figure 3.1.

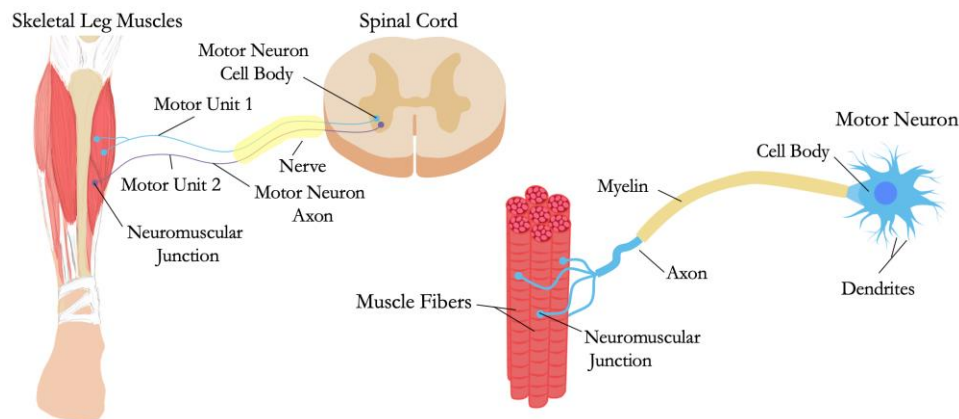


Figure 3.1: the motor unit

As the name suggests, spinal motor neurons reside in the spinal cord. Their main function is to receive incoming signals through their dendrites, perform signal integration in their cell body, and transmit the signal down their axon to the neuromuscular junction. As this signal travels down the axon an electrical signal known as an action potential (AP) is produced. A motor neuron and all the muscle fibers it innervates is a motor unit (MU). MU activation generates the force needed for the skeletal muscle contractions and relaxations that are responsible for moving and supporting the

skeleton. The intensity and duration of the contractions are determined by the recruitment and firing rate of the MUs. All the MUs within an individual muscle are classified as a motor pool. The combined process where various sensory inputs dictate certain motor outputs are commonly referred to as sensorimotor processes.

3.1.1.2. The Degrees of Freedom Problem

The musculoskeletal system is comprised of more than 200 skeletal bones and over 600 skeletal muscles, ligaments, and tendons. In order to generate movement each individual muscle requires the activation and coordination of thousands of individual MUs through their motor pools. This coordination to achieve a specific behavioral goal is inherently heavily redundant due to the degrees of freedom (DOFs) problem [25]. This problem suggests that redundancy arises from the infinite number of possible coordination patterns that generate the same movement goal. Simply put, the CNS has control over more musculoskeletal elements than possible musculoskeletal movements. Thus, a one-to-one correspondence between a specific movement task and a particular movement solution pattern cannot exist. Bernstein proposed a theory of hierarchical control where the CNS implements specific functional control structures to limit the DOFs at four-levels: muscle tone, muscle synergies, space, and actions [25], [26]. The organization of these muscle synergies are dictated by the constraints presented at the higher levels of environmental space and desired actions [26]. The actual neural mechanism used in the organization and coordination of musculoskeletal movement is not entirely known.

3.1.2. Neural Control Theories

3.1.2.1. Synergies

In the diverse field of motor control the term synergy has carried different connotations that are often not synonymous between various research approaches [27]. The simplest connotation for

muscle synergies are groups of muscles that act together to perform the same function [17]. The idea that muscle synergies are functional structures that contain the minimal number of muscle activations, needed to generate all movements within a behavioral goal is most persistent in neurophysiologic approaches [27]. Another interpretation rooted in neurophysiology holds that muscle synergies allow for the translation of task-level neural commands into execution-level muscle activation patterns [32]. These ideas are based on the CNS minimizing redundant DOFs.

Muscle synergies within the uncontrolled manifold (UCM) hypothesis stray from these more traditional views of minimizing DOFs. The UCM hypothesis suggests that the CNS achieves successful movement task performances by utilizing the abundant DOFs as elemental variables to create the most stabilized variable combination relevant to the present task [33], [34]. In this hypothesis synergies are organized as task-specific groups of DOFs that function to stabilize a particular performance objective [7]. Groups of muscles that function together to promote a movement task is the common theme surrounding synergies regardless of the goal to minimize or maximize redundant DOFs. How the CNS coordinates the activation of these functional synergies is unknown.

3.1.2.2. Common Neural Drive

Instead of individually activating each MU in a synergistic muscle group various studies suggest that neural control is simplified by the use of common neural drives that synchronously activate the motor pools of each muscle in the functional synergy as a signal unit at various frequencies. These studies propose that the CNS implements a common neural drive/input mechanism to coordinate the activation of synergistic muscle groups [6]–[19]. This proposition is based on the principle that neural oscillations are synchronized by the CNS to achieve large-scale integration among cortical and subcortical components that are involved in the control of muscle movement [6], [20]. A common neural drive that simultaneously activates multiple motor pools is

also synchronizing their firing rate [19]. The various frequency ranges that these neural drives oscillate at is indicative of their signal origin in the brain and are shown in Table 3.1

Table 3.1: Neural frequency bands and their known origin

Wave	Frequency (Hz)	Origin	Task Manifestation
Delta	0.5 – 4	Unknown	Isometric contraction, slow movements
Theta	4 – 8	Unknown	Isometric contraction, slow movements
Alpha	8 – 13	Unknown	Isometric contraction, slow movements
Beta	13 – 30	Motor cortex	Submaximal voluntary contraction
Lower Gamma	30 – 60	Motor cortex	Strong voluntary contraction, slow movements
Upper Gamma	60 – 100	Brainstem	Eye movement (60 – 90 Hz), respiration

The strength of neural synchronization from these frequency bands can be identified through the use of connectivity analysis from electromyography (EMG).

3.1.3. Human Balance and Postural Control

3.1.3.1. Balance, Stability, and Posture

Human balance refers to a state of equilibrium where a body’s center of pressure (COP) oscillates about its center of mass (COM) that is within the area of the base of support (BOS), made up of the feet to prevent a fall [1]–[3]. Stability is the inherent ability to maintain, achieve, and/or restore a balanced state in prevention of a fall [2]. If the COM becomes displaced and falls outside of the BOS, the body becomes unstable and thus unbalanced. COP is directly related to feet orientation. When only one foot is in contact with the ground the net COP is in that foot. When both feet are in contact with the ground the net COP is between the two feet and each foot has its own COP with respect to weight distribution [1]. Finally, posture describes the orientation of the multi-segmental human body relative to gravity [1]. These terms are often used interchangeably and in combination to assess and define stability in balance and posture of normal humans.

Humans are inherently unstable bipeds that need a continuously acting control system to maintain balance and stability due to their relatively large COM, located at two thirds of their body height above ground, and relatively small BOS [1], [4]. This postural control system is a complex motor skill coordinated by the central nervous system (CNS – i.e. brain and spinal cord) that integrates the interaction of multiple sensorimotor processes [2]. Failure of this system results in a loss of balance and stability which leads to an inevitable fall. The exact mechanism of how the CNS coordinates and regulates postural control is still relatively unknown.

3.1.3.2. Postural Control

Postural control is a learned complex motor skill organized by the CNS that adapts and integrates the interaction of multiple sensorimotor processes derived from an individual's expectations, goals, cognitive factors, and prior experiences [3]. The main function of postural control is to promote postural orientation and postural equilibrium of the multi-segmented musculoskeletal system by implementing either compensatory, or anticipatory, or a combination of both control strategies [4], [35]. Postural orientation involves the active control of the body's alignment with respect to gravity, support surface, sensory environment, and internal references while postural equilibrium refers to the coordination of the sensorimotor strategies used to stabilize the body's COM during internally and externally triggered perturbations or disturbances to balance [4].

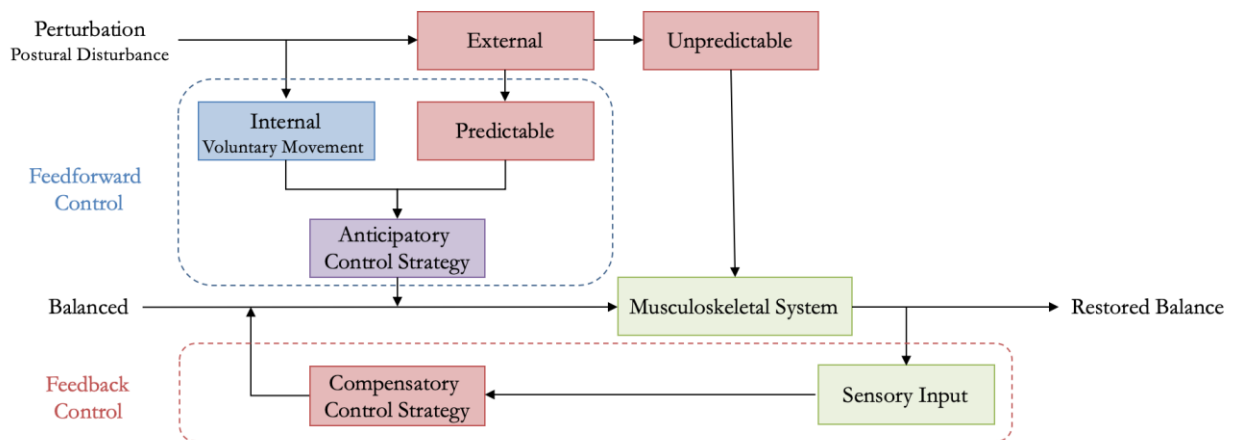


Figure 3.2 illustrates the conceptual model of postural control as it pertains to internal and external perturbations.

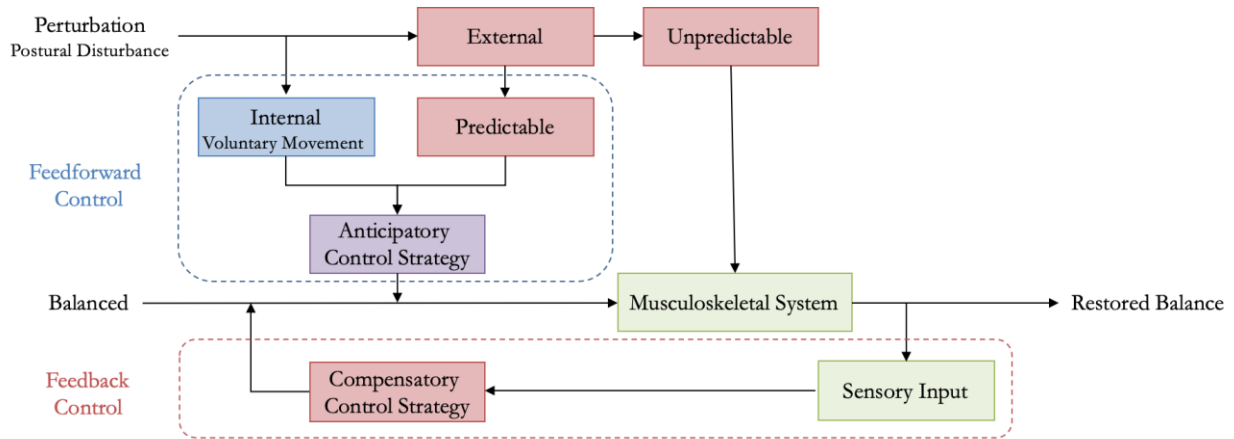


Figure 3.2: Simple conceptual model of postural control

This model shows that compensatory and anticipatory strategies are implemented following unpredictable and predictable perturbations respectively. Internal perturbations are caused by voluntary movement where only specific limbs of the musculoskeletal system are moved. During these movements neighboring musculoskeletal segments may become displaced and affect overall balance [4], [35]. The anticipatory movement strategy implements a feedforward control that predicts the amount of compensation needed to maintain stability, in advance, before the voluntary movements. External perturbations arise from unexpected changes to the sensory environment. The three main sensory systems involved in postural control are the visual, vestibular, and somatosensory systems.

These systems work together as a continuously active multisensory feedback control system, that actively reweighs sensory input, to elicit the immediate compensatory strategy needed to combat changes in the sensory environment [4], [24]. This ability to re-weight sensory information depending on the sensory context is important for maintaining balance and stability relative to the present sensory environment [4]. Damage to any one of these systems will lead to difficulties in proper allocation of sensory weights. The effects of external perturbations becomes predictable after

repeated implementation. When this happens, the known compensatory strategy shifts into an anticipatory strategy.

Both anticipatory and compensatory control strategies involve the use of either a “fixed-support”, or a “change-in-support”, or both movement strategies depending on if the subsequent limb movement used to regain balance alters the BOS [35]. Commonly defined “fixed-support” strategies are the ankle and hip strategies, while stepping and grasping/reaching with a hand are common “change-in-support” strategies as shown Figure 3.3.

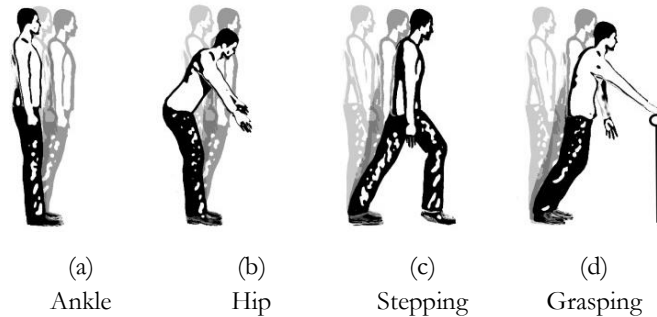


Figure 3.3: Postural control strategies

“Fixed-support” strategies do not alter the BOS. The ankle strategy (Figure 3.3a) is able to maintain balance by counteracting small perturbations, when standing on a firm surface, by adjusting only the ankle plantar/dorsiflexor muscles. These muscles are listed in Table 3.2 and are denoted with either (P) for plantarflexors or (D) for dorsiflexors.

Table 3.2: Plantarflexor (P) and dorsiflexor (D) muscles of the lower legs

Posterior Muscles	Anterior Muscles	Deep Anterior Muscles
Medial gastrocnemius (P)	Tibialis anterior (D)	Tibialis posterior (P)
Lateral gastrocnemius (P)	Fibularis longus (P)	Flexor digitorum longus (P)
Plantaris (P)	Extensor digitorum longus (D)	Flexor hallucis longus (P)
Soleus (P)	Fibularis brevis (P)	
	Extensor hallucis longus (D)	

In the event that the COM shifts significantly, and the ankle strategy is unable to compensate the perturbation, the hip strategy (Figure 3.3b) is then used to either flex or extend the

hips to realign the COM with the BOS [1], [35]. When maintaining a fixed BOS is not necessary the “change-in-support” strategies, specifically stepping (Figure 3.3c) are commonly used in the recovery of balance.

3.1.3.3. *Clinical Implications*

Cognitive, sensory, or motor impairments due to aging, injury, neurological disorders, and traumatic brain injuries may create deficits in the postural control system. Recognizing the pathophysiological and degenerative neurological changes, from these impairments, is central to understanding the causes and consequences of balance disorders and their clinical management [35]. Significant knowledge surrounding the postural control system and its impairments has been gained from balance perturbation studies comparing how both healthy and impaired individuals respond to externally imposed challenges to stability [14], [18], [21], [24], [35].

3.1.4. **Quiet Standing**

3.1.4.1. *Overview of Quiet Standing*

Maintaining quiet, upright bipedal stance is a fundamental activity of daily human life. The Center for Disease Control’s (CDC) Stopping Elderly Accidents, Deaths, and Injuries (STEAR) initiative evaluates balance using a four-stage functional assessment balance test [36]. The feet orientation for each standing position becomes progressively harder to maintain and are shown in Figure 3.4.

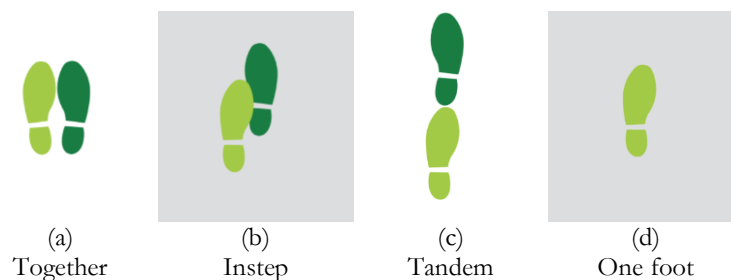


Figure 3.4: 4-stage functional assessment balance test positions [36]

Feet together is the easiest of the bipedal stances to maintain while feet tandem is considered the hardest. If an older adult is unable to hold the tandem feet position for a minimum of 10 seconds, they are then considered to be at an increased risk of falling [36].

The biomechanical models most commonly used to explore how the CNS implements postural control in quiet standing are the inverted pendulum models. The two most widely recognized inverted pendulum model are the single inverted pendulum (SIP) and the double inverted pendulum model (DIP) and are illustrated in Figure 3.5.

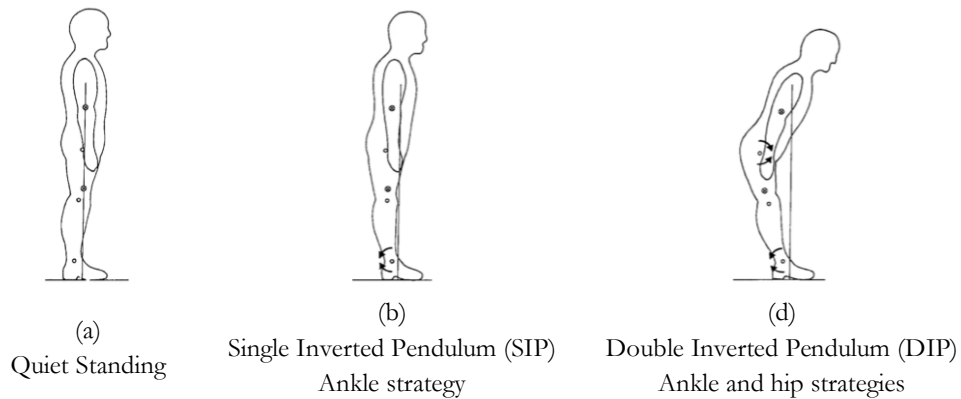


Figure 3.5: Inverted pendulum models and their postural control strategies adapted from [1]

Humans, as bipeds, are unable to stand completely still during quiet stance due to the continuous oscillation of their COP around the COM. These oscillations, commonly referred to as postural sway, are needed to maintain a balanced distribution of COM between the BOS and occur in the anterior-posterior (AP) and medio-lateral directions (ML) [37], [38]. The measured displacement of these oscillations patterns provides an indirect estimation of postural sway in the context of both SIP and DIP inverted pendulum models [38].

3.1.4.2. Inverted Pendulum Models

The inverted pendulum models were proposed to explain how the inherently unstable human is able to maintain balance. These models are quantified by the ‘fixed-support’ movement

strategies the CNS employs in the stabilization and recovery of balance (Figure 3.5). This model employs only the use of the ankle strategy. However, various studies have identified non-negligible hip movement in quiet standing and thus a combined ankle-hip strategy as a DIP model should be employed [1], [5]. In quiet standing with feet together the ankle strategy dominates in the AP (front-to-back) direction while a separate hip strategy dominates in the ML (side-to-side) direction [1]. When the feet are in tandem stance it was found that the two strategies reverse roles with the ankles working in the ML direction and the hips in the AP direction [1]. Although the SIP model is considered an over-simplification of postural control it is functionally correct in its assumption that ankle movement is more prevalent in quiet bipedal stance [5].

3.1.4.3. Postural Sway

Postural sway refers to the seemingly spontaneous sways of the human body during quiet stance caused by oscillations in the COP about the COM. The location of the COP under each foot, with respect to feet orientation, is a direct reflection of the neural mechanisms of the ankle muscles in postural control [1], [38]. Studies have shown that postural sway is influenced by changes in the sensory environment and lower leg muscle activation [24], [39]. Impairments to vision had the greatest effect, by increasing sway, among the sensory systems [24]. Increased muscle activation of the lower leg muscles was found to decrease sway [39]. One study theorized that postural sway was an exploratory mechanism used by the CNS to ensure continuous dynamic inputs were being provided by the multisensory system [37]. The exact cause and purpose of postural sway is still relatively unknown.

3.1.5. Connectivity

3.1.5.1. EMG

EMG measures the electrical activity of skeletal muscles during muscular contraction dictated by the CNS. Surface electrodes are most commonly used for EMG measurements. They are placed directly on the skin and the resultant EMG signal is a composite of all the muscle fiber action potentials in the muscles that lie directly under the skin [40]. The combination of the muscle fiber action potentials from all the muscle fibers of a single motor unit is the motor unit action potential (MUAP), which can be detected by a surface electrode [40]. An EMG signal is a train of MUAPs representing a muscle response elicited from a neural drive [40]. Thus, the shape and firing rate of MUAPs in EMG signals gives valuable information about how the CNS coordinates muscle activation. Increased MUAP recruitment is directly related to increased muscle force and activation. This distinct relationship between CNS control and muscular activation allows for the indirect extraction of synaptic input signals received by the motor neurons from EMG signals [22].

3.1.5.2. Functional Connectivity

Connectivity analysis methods take advantage of the indirect measure of neural drive within EMG signals. The existence of synchronous neural drives can be deduced from comparing intermuscular coherence between various EMG signals of muscles within a similar functional. The EMG signals of postural control muscles used to maintain quiet standing could provide valuable information about the underlying neural mechanism of postural control. Numerous studies have used intramuscular (EMG-EMG) coherence analysis to identify synchronization and common neural drive to various muscles during various postural control standing tasks [6]–[19]. These studies found that high coherence at specific frequencies between postural control muscles could indicate whether or not a common neural drive was acting on them. The use of coherence analysis provides useful information regarding the neural mechanism used by the CNS for postural control.

High coherence in the delta band has been commonly observed in the lower legs' anterior and posterior M-modes during quiet standing, which reflects possible subcortical/spinal inputs as well as co-modulation of muscle activation [9], [12], [33]. The actual origin of delta bands is unknown but manifests during isometric actions [34]. Coherence in the theta and alpha bands reflect possible subcortical and corticospinal inputs manifesting in isometric contractions and slow movements during various postural control tasks [9], [10], [34]. A 10 Hz coherence peak was found between same leg posterior muscle pairs when vision was compromised [10]. Coherence in the beta and lower gamma (30 – 60 Hz) bands reflect motor cortex origins [34]. Postural control is a motor task thus, some amount of coherence should be expected during quiet standing in these bands. The upper gamma band has been found to be associated with eye movement and respiration oscillatory drives [34]. Previously mentioned studies examining standing task postural control did not examine coherence past the lower gamma band.

3.2. Extended Methodology

3.2.1. Participants

All subjects were considered healthy with no history of neurological or muscular disorders. Exemptions included: history of head trauma that resulted in a loss of consciousness, history of musculoskeletal injuries to the trunk and/or lower extremities that required reconstructive surgery, and any non-weight bearing injury to the lower extremities in the past 12 months. Subjects were asked to fill out an informative questioner to gauge their current activity level as well as gauge how their sports history could contribute to their postural control system. The following anthropometric measures of body height (cm), mass (kg), inter-anterior superior iliac spine (ASIS) distance (cm), and both right and left leg length (cm), knee width (cm), and ankle width (cm) were collected prior to subject preparation. These measurements are needed to normalize the calculated outputs of the Full-Body Plug-in-Gait (FB PiG) model used for motion capture analysis to the subject. Table 3.3 shows the individual characteristics of each subject.

Table 3.3: Participant characteristics

Subject	Gender	Foot Dominance	Age	Height (cm)	Weight (kg)
SB01	F	Right	26	170.4	64.5
SB02	F	Right	21	162.6	64.7
SB03	M	Left	23	174.7	63.9
SB04	M	Left	28	190	98.2
SB05	F	Right	25	163	70.1
SB06	F	Right	25	164	63.2

3.2.2. Experimental Procedure

Subjects were asked to perform a static trial by holding the anatomical position of feet shoulder width apart, arms slightly raised at the sides, and palms and head facing forward for one second prior to starting the experiment protocol. The purpose of the static trial was to calibrate a Vicon labeling skeleton (VSK) from an existing Vicon skeletal template (VST) which would enable

NEXUS to automatically detect and recognize the subject and determine the proper reconstruction labels for subsequent trials following the static trial. Combined with the anthropometric measurements of each subject the calibration process is able to calculate body segments, joint centers, and determine a local reference system for dynamic calculations. Following the static trial subjects began the experiment protocol in the order listed in Table 3.4.

Table 3.4: Quieting standing balance conditions

Condition	Order	Description
EOFT	1	Eyes open, feet together
ECFT	2	Eyes closed, feet together
EOTanDB	3	Eyes open, feet tandem, dominant foot in back
ECTanDB	4	Eyes closed, feet tandem, dominant foot in back
EOTanDF	5	Eyes open, feet tandem, dominant foot in front
ECTanDF	6	Eyes closed, feet tandem, dominant foot in front

EOFT stance was assumed to be the most stable condition. This condition was completed first to ensure a proper baseline measure would be collected to compare the other less stable conditions against. The other conditions were completed in the order they are listed. In order to limit possible effects of fatigue and allow standardization between different subjects a 30 second break was implemented between trials and a 2-minute break between each condition. Subjects were encouraged to sit during the 2-minute break to ensure full recovery of any underlying fatigue. Before the start of each tandem stance trial subjects were made aware of their COP distribution between their feet and were asked to achieve equal distribution. Once the trial started subjects did not receive further encouragement in maintaining equal distribution.

In the event that the subject felt they were losing balance they were instructed to immediately rectify their loss of balance and resume the testing stance. The use of stepping, arm motions, hip, and ankle strategies were expected. Trials were redone if subjects moved their feet off the designated force plates illustrated in Figure 3.6.

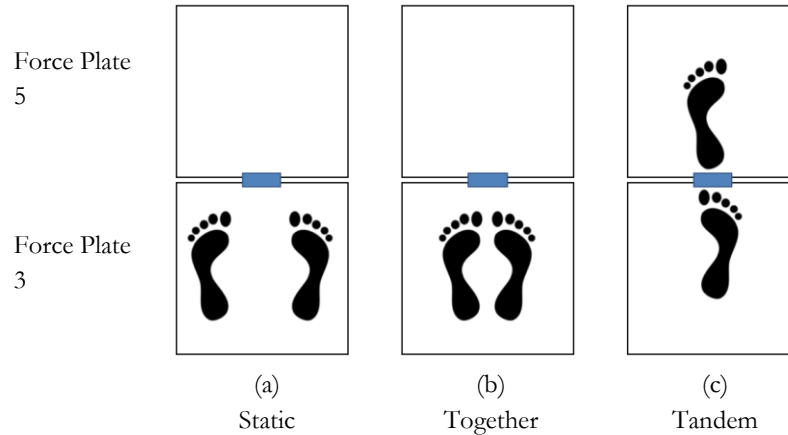


Figure 3.6: Feet orientation

The width of 1.5-inch athletic tape (shown as the blue rectangle in Figure 3.6) was used as an indicator of the junction between both force plates. Subjects were instructed to position the toe of the back foot and heel of the front foot on the outside edges of the tape. The use of the tape ensured that individual COP oscillations of each foot was being collected independently. It also ensured standardization amongst the different subjects.

3.2.3. Data Acquisition

3.2.3.1. Subject Preparation

Subjects were informed before data collection that their lower legs had to be bare of hair to minimized potential noise sources to the EMG signal. The placement of the MA-411 pre-amplifiers (Motion Lab Systems Inc., Baton Rouge, LA) on the tibialis anterior (TA), medial gastrocnemius (MG), and soleus (S) of the right (R) and left (L) legs is indicated in Figure 3.7.

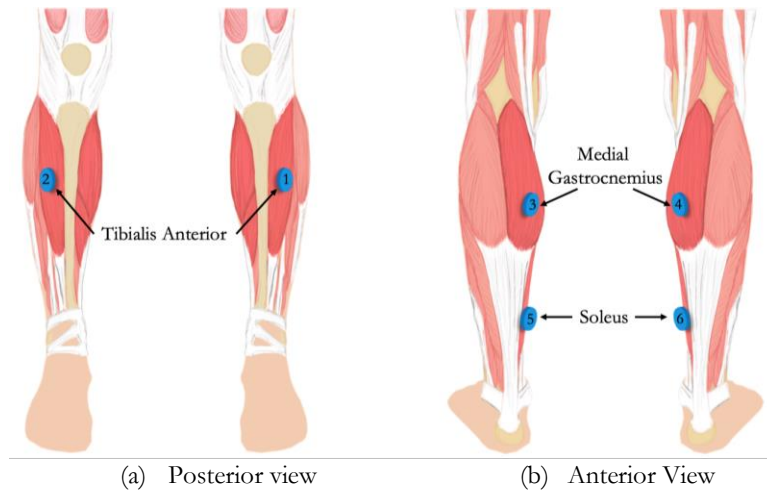
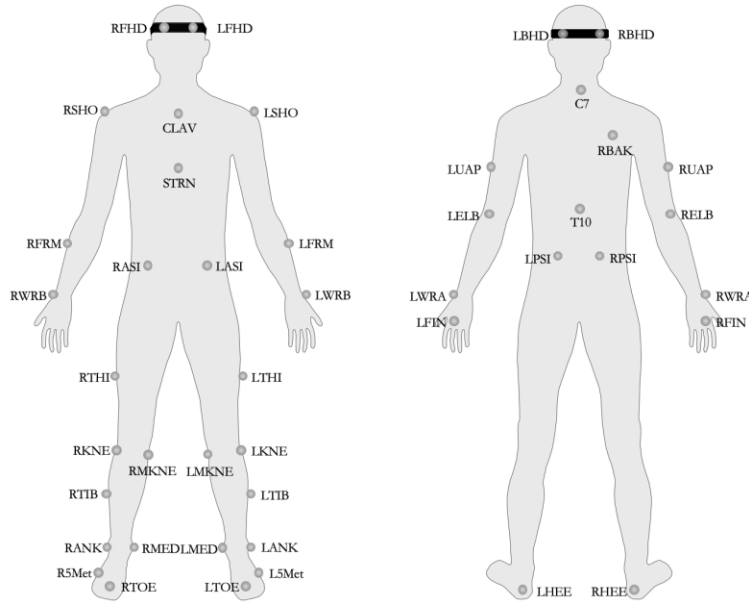


Figure 3.7: Pre-amplifier placement

The skin directly below the location of the pre-amplifiers was prepped using alcohol swabs, and abrasive sponge pads to remove any dead skin that would impede proper electrode-skin contact. The preamplifiers were placed directly over the belly of the muscles of interest parallel to the orientation of the muscle fibers. 3M hypoallergenic tape was used to secure the preamplifiers in place. Subjects were asked to generate plantar/dorsiflexion movement by going on their toes and heels to ensure signal integrity of the MG and S plantarflexors and TA dorsiflexor respectively. Pre-wrap was used to wrap the entire calf to secure the preamplifiers and their cables in place in order to minimize possible motion artifacts from cable movement.

Following pre-amplifier placement, the subject underwent marker placement of the modified Full-Body Plug-in-Gait model for motion capture. Figure 3.8 illustrate the location of the markers in this model during static stance. The modified model included the addition of the fifth metatarsal (5th – Met) and a medial knee marker in place of the knee alignment device. The FB PiG 5th – Met model was a predefined biomechanical model used solely for the purpose of this study. Markers were secured to their proper anatomical locations using double sided hypoallergenic tape and 3M tape.

Head	
FHD	Forehead
Upper Limb	
SHO	Shoulder
FRM	Forearm
WRB	Wrist Marker B
Torso	
CLAV	Clavicle
STRN	Sternum
Pelvis	
ASI	Anterior Superior Iliac
Lower Limb	
THI	Thigh
KNE	Knee
TIB	Tibia
ANK	Ankle
MED	Medial Malleoli
TOE	Toe
Modified Markers	
MKNE	Medial Knee
5Met	5 th Metatarsal



Head	
BHD	Back of Head
Upper Limb	
UAP	Upper Arm
ELB	Elbow
WRA	Wrist Marker A
FIN	Finger
Torso	
C7	7 th Cervical Vertebra
BAK	Right Back
T10	10 th Thoracic Vertebra
Pelvis	
PSI	Posterior Superior Iliac
Lower Limb	
HEE	Heel

Figure 3.8: Modified Full-Body Plug-in-Gait model

3.2.3.2. Instrumentation

6 MA-411 pre-amplifiers were interfaced with the MA300-XVI EMG patient unit acquisition system (Motion Lab Systems Inc., Baton Rouge, LA) at a 1200 Hz sampling frequency. The MA300 patient unit has a fixed 10 – 1000 Hz (-3dB) bandwidth and uses a 500 Hz low-pass anti-aliasing filter. The MA-411 pre-amplifiers have an input impedance greater than 100,000 M Ω a gain of 1 kHz x 20 \pm 1%, a common mode rejection ratio (CMRR) greater than 100 dB at 65 Hz, and noise less than 1.2 μ V root mean square (RMS). The analog EMG signals were high passed filtered at 10 Hz by the active Motion Lab System unit. Gains were adjusted on a subject by subject basis to prevent signal clipping.

Two floor-embedded AMTI (Advanced Mechanical Technology Inc., Watertown, MA) force plates were used to measure the forces and moments applied during quiet standing. Ground reaction forces were collected at a sampling frequency of 1200 Hz. Real time observation of vertical force vectors helped to see if subjects were able to maintain an equal distribution between their feet during the various feet orientations (Figure 3.6). Movement trajectories of the musculoskeletal system were

tracked using sixteen VICON motion capture cameras. EMG, force plate, and motion capture data were synchronized using Nexus motion capture software v2.8 (Oxford Metrics, Oxford, UK). Only EMG data were used for further analysis.

3.2.4. Data Analysis

All recorded EMG signals were analyzed using frequency analysis methods to observe functional connectivity between unilateral and bilateral homologous muscle pairs using MATLAB R2018a (The MathWorks, Natick, MA). Neural frequency band activity occupies the 0 – 100 Hz range. A sampling frequency of 1200 Hz gives rise to a 0 – 600 Hz usable frequency range that satisfies Nyquist's Theorem. The 0 – 450 Hz range of raw EMG signals is known to contain the most activity. A 4th – order lowpass Butterworth filter was applied at 450 Hz.

3.2.4.1. Preprocessing

EMG signals are inherently noisy, but many sources of noise can be easily identified and reduced. One of the easiest signal noises to identify is power line interference (PLI) that exists at 60 Hz. A notch filter is commonly used to remove PLI. Removal of PLI with a notch filter will also remove and distort valuable spectral information. PLI exists in the middle of the gamma band. By splitting the gamma band around the PLI distortion the effect of the distortion is now around the edge of the frequency ranges instead of the middle. With this in mind a 2nd – order Butterworth notch filter at 60 Hz with a 0.2 Hz bandwidth filter was applied to remove the PLI. Overall signal distortion was found to be minimal in the whole gamma band. When the gamma band is split these minimal distortions were present on the edges. These distortions were smoothed out in later signal analysis methods.

The 0 – 20 Hz frequency range is known to contain noise due to motion artifacts (0 – 10 Hz), motor unit firing (0 – 20 Hz), and skin conductance (0 – 1 Hz) [40]. These noises overlap with the frequency contents of the lower neural frequency bands and part of the beta band. Possible motion artifacts due to movement of EMG cables was minimized by implementing pre-wrap to hold down the wires on each subject. MATLAB’s Welch’s power spectral density estimator was used to visually analyze presence of low frequency noise across the EMG signals of baseline (EOFT) condition. A 0.8 Hz harmonics with varying amplitudes was found to exist in all preamplifiers with the strongest power in the LTA, RTA, LMG, and RMG among all subjects. However not enough information could be concluded about this harmonic to fully remove it as signal noise. Further preprocessing to remove these noises was not implemented for fear of losing the neural components that exists in the 0 – 20 Hz range.

3.2.4.2. *Magnitude Squared Coherence*

Magnitude squared coherence (MSC) measures the linearity of the phase relation between two signals x and y in the frequency domain defined by

$$C_{xy} = \frac{|S_{xy}(f)|^2}{S_{xx}(f)S_{yy}(f)} \quad (3.1)$$

where C_{xy} is MSC, S_{xy} is the cross-spectrum power and S_{xx} and S_{yy} are the auto-spectrums of input signals x and y at frequency f . MSC values are evaluated between 0 and 1, where 0 indicates no linear relationship and 1 is a perfect linear relationship between input signals x and y at frequency f . The use of intermuscular coherence provides insight into the relationship between EMG signals of neighboring leg muscles. These muscles could be grouped by their role in ankle movement as planter/dorsiflexors, their agonistic or antagonistic relationship, or if they belong to

the same synergistic M mode. Coherence has been found to be indicative of these relationships [14], [19].

MATLAB has a built in MSC function that estimates C_{xy} using Welch's overlapped periodogram method. MSC was estimated for all filtered data sets across each muscle and condition using MATLAB's MSC function using a two-second Hamming window, with 25% overlap. This created 19 window segments of 2400 data points and a frequency resolution of 0.5 Hz. This frequency resolution was chosen because it provided the best estimate while preserving the trade-off between time and frequency. A total of 9 muscle pairs were identified between the L/RTA, L/RMG, and L/RS. Only unilateral muscles of the same leg and bilateral muscles of the same type were compared.

The gamma band was previously split due to the existence of the PLI. Most studies that looked at intermuscular coherence only looked up to 50 – 60 Hz in the gamma band [13], [15], [16], [19]. Thus, by splitting gamma band into two parts the lower gamma band results can be compared to existing literature. Each neural frequency range was averaged across its MSC spectrum to generate a singular coherence value for that range. Average was chosen over median in order to preserve the presence of various frequency spikes in the MSC spectrum. In this case outliers should not be excluded since they give valuable information about possible underlying common neural drive mechanisms involved in postural control.

3.2.4.3. *Mutual Information*

Mutual information (MI) is an information theory measurement that measures the information dependence between two random variables. Specifically, it quantifies how much information two time series X and Y share with one another. This measure is rooted in entropy, or degree of uncertainty, in a time series X defined as

$$H(X) = - \sum_{i=1}^n p(x_i) \log_2 p(x_i) \quad (3.2)$$

where X is a discrete random variable and $p(x_i)$ is the probability mass function of X .

When working with two time series X and Y joint and conditional entropies can be derived. Joint entropy refers to the measure of uncertainty associated with time series X and Y defined as

$$H(X, Y) = - \sum_x \sum_y p(x, y) \log_2 p(x, y) \quad (3.3)$$

where $p(x, y)$ is the joint probability of particular values x and y occurring together.

Condition entropy of a random variable X based on the conditional knowledge of another variable Y is defined as

$$H(X|Y) = - \sum_x p(x) \sum_y p(x|y) \log_2 p(x|y) \quad (3.4)$$

and can be rearranged so that conditional entropy is based on the joint probability of $p(x, y)$ and the conditional probability $p(x|y)$

$$H(X|Y) = - \sum_x \sum_y p(x, y) \log_2 p(x|y) \quad (3.5)$$

The relationship between joint and conditional entropy are related such that

$$H(X, Y) = H(X) + H(Y|X) \quad (3.6)$$

The relative entropy known as the Kullback – Leibler divergence, or information gain, measures the distance between two distributions and is defined as

$$D(p||q) = \sum_x p(x) \log \frac{p(x)}{q(x)} \quad (3.7)$$

and is always non-negative [29]. The relative entropy of joint distribution $p(x, y)$ and the product distribution of $p(x)p(y)$ is called mutual information and is written such that

$$I(X, Y) = \sum_x \sum_y p(x, y) \log_2 \frac{p(x, y)}{p(x)p(y)} \quad (3.8)$$

When simplified into its entropy components MI provides a measure of the amount of information that Y contains about X and provides a reduction of uncertainty between X and Y when given Y .

$$I(X, Y) = H(X) - H(X|Y) = H(X) + H(Y) - H(X, Y) \quad (3.9)$$

Unlike MSC, MI does not assume any dependence properties between two signals such as linearity and therefore is able to provide more general estimates of connectivity between signals. MI not only gives information about dependence but also infer independence between two signals if MI is 0 unlike coherence at 0 [28].

MI is viewed as information gain and a reduction of uncertainty. High MI is indicative a high reduction of uncertainty and zero MI indicates that the two time series are completely independent of one another. Another way to view MI is quantifying that future values of X can be better predicted from also knowing past values of Y and not just relying on the past values of X . The value assigned to MI are unique to the specific times series that are being compared. Thus, in order to compare across multiple comparisons MI must be normalized. The normalization method that was employed was described by Michaels et al. in the context of analyzing large-scale gene expression and is defined as

$$I_{NM}(X, Y) = \frac{I(X, Y)}{\max(H(X), H(Y))} \quad (3.10)$$

where MI is normalized in the 0 to 1 range based on the maximal entropy of each contributing time series [31]. Michaels et al. used this normalization method because the degree of mutual information was dependent on how much entropy was carried by each gene expression sequence. A gene expression sequence pair exhibiting low information entropies will also have low MI, even if they are completely correlated [31].

MI was obtained using the MIDER toolbox for MATLAB created by Villanverde et al. [29]. In this toolbox the probability distribution was estimated using an adaptive binning method based on the adaptive partitioning method proposed by Cellucci et al. [41]. In normal probability distribution methods bins are chosen to be of equal size. Problems arise when each bin contains unequal numbers of data points. Adaptive binning ignores uniform bin size for uniform number of data points across bins. The MIDER toolbox also includes the ability to implement Michaels et al. normalization.

MI was calculated between the same 9 muscle pairs MSC was. In order to make MI comparable to MSC sEMG data sets were manipulated similar to how MSC was calculated. 4th order Butterworth lowpass and bandpass filters were applied to the sEMG signals to view only the signals present in each of the neural frequency bands of interest. The delta band implemented the lowpass filter with a 4 Hz cut-off. The other frequency bands used bandpass filters with cut-off frequencies at their listed band range. MSC was averaged using a sliding average of 2400 data points with a 25% overlap. For calculating MI MIDER was implemented over 2400 data point segments with 25% overlap to create 19 segments for MI. The average MI of the 19 segments was used.

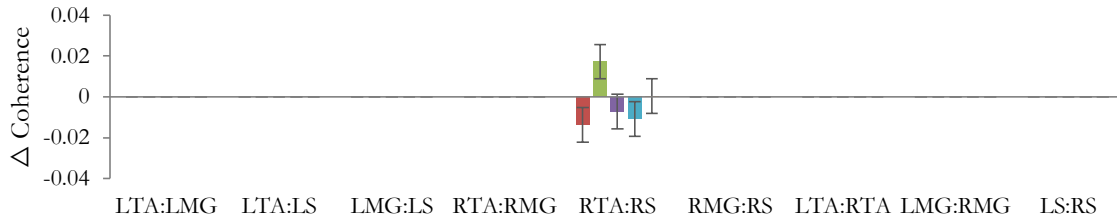
SB01

One-way ANOVA returned no significance

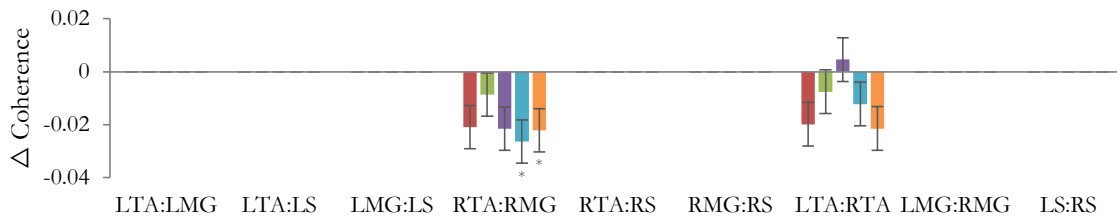
SB02

One-way ANOVA returned no significance

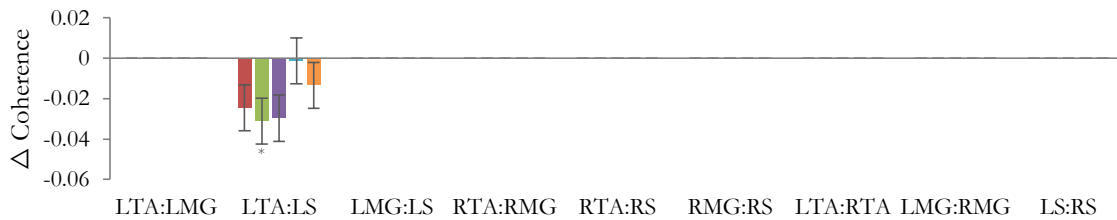
SB03



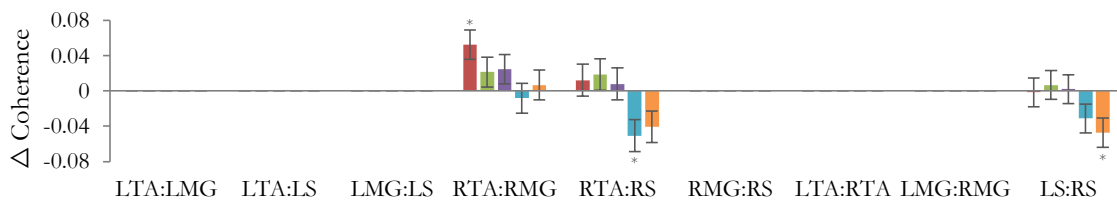
SB04



SB05



SB06



■ ECFT ■ EOTanDB ■ ECTanDB ■ EOTanDF ■ ECTanDF

Figure A.2: Results of Dunnett's two-sided post-hoc t-test for multiple comparisons against baseline (EOFT) condition for significant MSC in the theta band

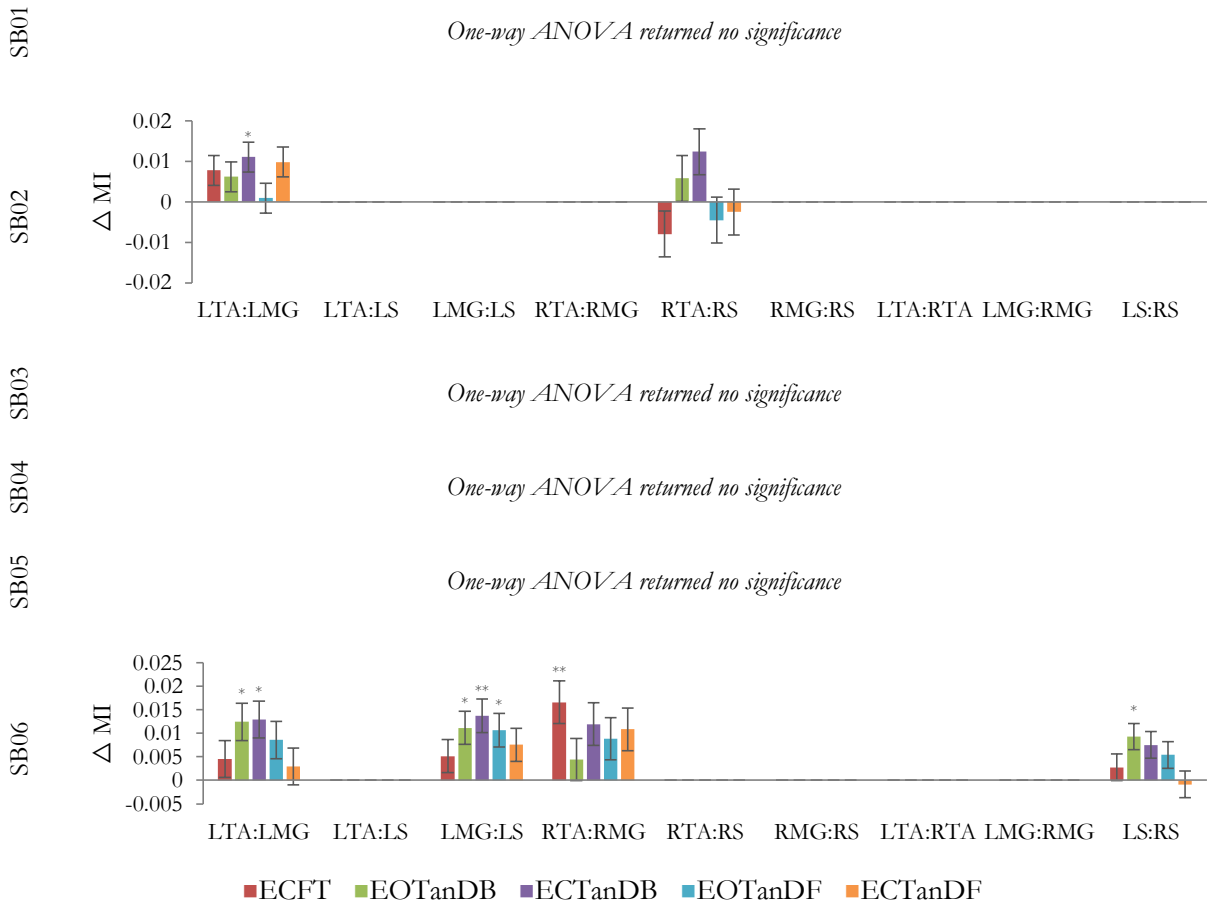
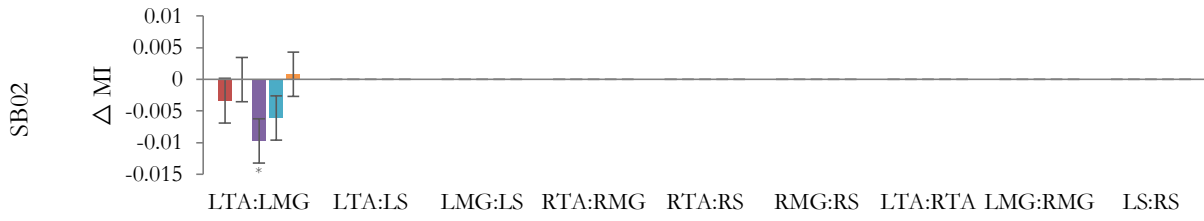


Figure A.3: Results of Dunnett's two-sided post-hoc t-test for multiple comparisons against baseline (EOFT) condition for significant MI in the delta band

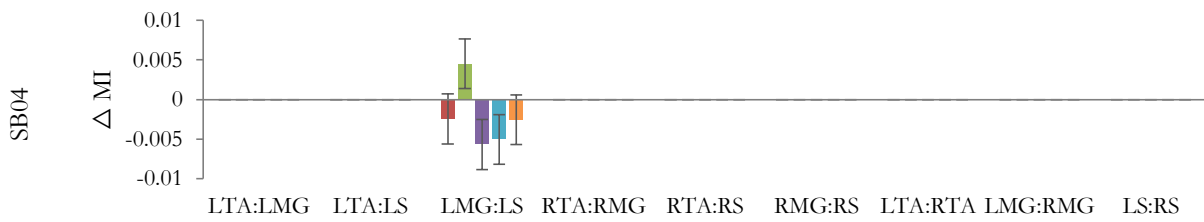
SB01

One-way ANOVA returned no significance

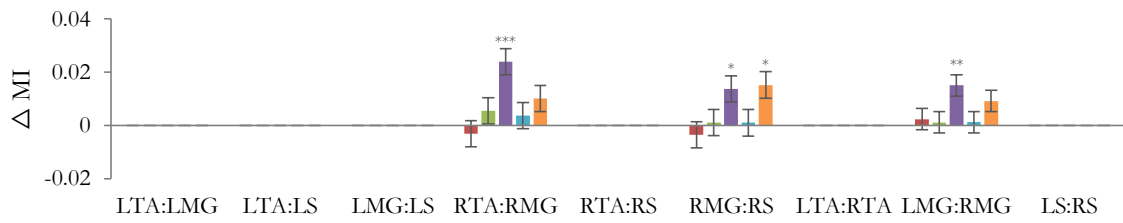


SB03

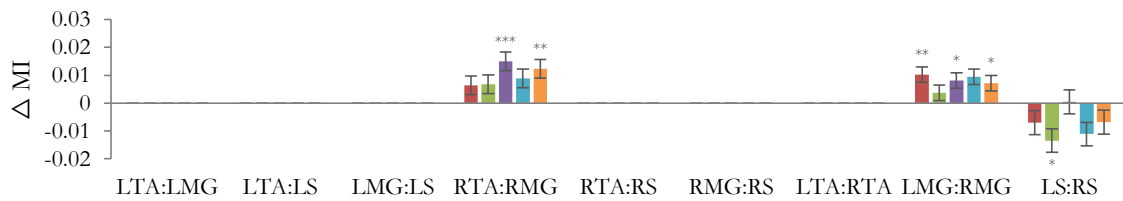
One-way ANOVA returned no significance



SB05



SB06



■ ECF Γ ■ EOTanDB ■ ECTanDB ■ EOTanDF ■ ECTanDF

Figure A.4: Results of Dunnett's two-sided post-hoc t-test for multiple comparisons against baseline (EOFT) condition for significant MI in the theta band

Appendix B. Code

B.1. Preprocessing of EMG Signals

```
%%%%%%%%%%%%%%%%%%%%%%%%%%%%%%%%%%%%%%%%%%%%%%%%%%%%%%%%%%%%%%%%%%%%%%%%
% Title: Load_Data.m
% Author: Diana McCrumb
% Notes: this script file loads all subject data into a usable structure
% for further analysis.
% 1. data is z-score normalized
% 2. 60 Hz powerline interference removal filter
% 3. 450 Hz low pass filter
%%%%%%%%%%%%%%%%%%%%%%%%%%%%%%%%%%%%%%%%%%%%%%%%%%%%%%%%%%%%%%%%%%%%%%%%
close all; clear all;

% for loop to cycle through all usable subjects data sets
for s = 1:6
    [fname,pname] = uigetfile({'*.csv'},'Select EMG File','MultiSelect','on');
    filename = fullfile(pname, fname);

    for z = 1:30
        raw_data(:, :, z) = csvread(filename{z}, 5, 2, [5, 2, 36004, 7]);
    end

    norm_data = normalize(raw_data(:, :, :), 1);           % normalize data sets
    % 60 Hz notch filter
    dnotch = designfilt('bandstopiir', 'FilterOrder', 6, ...
        'HalfPowerFrequency1', 59.9, 'HalfPowerFrequency2', 60.1, ...
        'DesignMethod', 'butter', 'SampleRate', 1200);
    notch_data = filtfilt(dnotch, norm_data(:, :, :));

    % 450 Hz low pass filter
    fc = 450;           % set cut off frequency
    w = fc/600;        % normalize cut off frequency
    [b,a] = butter(4,w,'low');           % design filter
    lpass_data = filtfilt(b,a,notch_data(:, :, :)); % apply filter

    % save data into useable structure
    %SB_Data(s).Loaded = lpass_data;
    SB_Data(s).Loaded = lpass_data;
end
% save subject data in a usable structure for later use
file_name = sprintf('FB_Subject_Data.mat'); save(file_name, 'SB_Data')
```

B.2. MSC Calculation

```
%%%%%%%%%%%%%%%%%%%%%%%%%%%%%%%%%%%%%%%%%%%%%%%%%%%%%%%%%%%%%%%%%%%%%%%%
% Title: MSC.m
% Author: Diana McCrumb
% Notes: this script file calculates the MSC for the filtered EMG with
% with 25% overlap
% 1. Calculate MSC for each muscle pair of interest between:
% (1) LTA, (2) RTA, (3) LMG, (4)RMG, (5)LS, (6)RS
% 2. Average MSC over frequency range of interest
%%%%%%%%%%%%%%%%%%%%%%%%%%%%%%%%%%%%%%%%%%%%%%%%%%%%%%%%%%%%%%%%%%%%%%%%
% calculate MSC with 25% overlap

close all; clear all;
load Subject_Data.mat
```

```

fs = 1200; % sampling frequency
noverlap = 600; % 25% overlap
Wn = 2400; % 4 second window for 0.5Hz frequency resolution

pairs = {1,1,3,2,2,4,1,3,5;... % x
         3,5,5,4,6,6,2,4,6}; % y

for s = 1:6 % loop through all subjects
    data = SB_Data(s).Loaded;
    for z = 1:30 % all trials
        for p = 1:9 % necessary muscle pairs
            x = data(:,pairs{1,p},z); % x
            y = data(:,pairs{2,p},z); % y

            [cxy(:,p,z),f] = mscohere(x,y,hamming(Wn),noverlap,Wn,fs);
            SB_Data(s).MSC = cxy;
        end
    end
end
save('Subject_Data.mat', 'SB_Data','-append');

%% Average MSC spectrum for each condition for each subject from 0 - 100 Hz
close all; clear all;
load Subject_Data.mat

for s = 1:6 % subjects
    data = SB_Data(s).MSC;
    % separate trials into conditions
    [x,y,z] = size(data);
    C = mat2cell(data,x,y,5*ones(1,6));
    C = C(:);
    for k = 1:6 % conditions
        temp = C{k,:};
        temp_mean(:, :, k) = mean(temp,3);
    end
    SB_Data(s).Mean_MSC_Spectrum = temp_mean;
end
save('Subject_Data.mat', 'SB_Data','-append');

%% average MSC at each frequency band for each subject and each condition/trial
close all; clear all;
load Subject_Data.mat

bands = {'Delta','Theta','Alpha','Beta','Lower_Gamma','Upper_Gamma'}; % frequency band
range = {[1:9],[9:17],[17:27],[27:61],[61:121],[121:201]}; % frequency band ranges

for s = 1:6 % subject
    data = SB_Data(s).MSC;
    for b = 1:numel(bands); % loop through frequency bands
        band = range{1,b};
        temp = data(band, :, :);
        temp_mean(:, :) = mean(temp,1);
        data_mean(:, :, b) = temp_mean;
        SB_Data(s).Mean_MSC_FB = data_mean;
    end
end
save('Subject_Data.mat', 'SB_Data','-append');

```

B.3. *Mutual Information*

```
%%%%%%%%%%%%%%%%%%%%%%%%%%%%%%%%%%%%%%%%%%%%%%%%%%%%%%%%%%%%%%%%%%%%%%%%
% Title: MI.m
% Author: Diana McCrumb
% Notes: this script file computes MI for each filtered EMG signal
% 1. Filter EMG into frequency band ranges
% 2. Average EMG data with 25% overlap
% 3. Apply MIDER toolbox
%%%%%%%%%%%%%%%%%%%%%%%%%%%%%%%%%%%%%%%%%%%%%%%%%%%%%%%%%%%%%%%%%%%%%%%%
close all; clear all;
load Subject_Data.mat

% filter data into frequency bands

n = 4; % filter order
fs = 1200; hfs = 600; % sampling frequency and half frequency
bands = {'Delta', 'Theta', 'Alpha', 'Beta', 'Lower_Gamma', 'Upper_Gamma'}; % frequency band
filter_type = {'low', 'bandpass', 'bandpass', 'bandpass', 'bandpass', 'bandpass'};
FC = {4, [4 8], [8 13], [13 30], [30 60], [60 100]}; % cut off frequency

for s = 1:6 % subject
    data = SB_Data(s).Loaded;
    for b = 1:numel(bands) % bands
        fc = FC{1,b}; % cut off frequency
        Wn = fc/600;
        [z,p,k] = butter(n,Wn,filter_type{b}); % create filter
        [sos,g] = zp2sos(z,p,k);
        FB_Data(s).(bands{b}) = filtfilt(sos,g,data); % apply filter
    end
end

% use mider to calculate MI for data sets and store into an array
variables = {'LTA', 'RTA', 'LMG', 'RMG', 'LS', 'RS'};

npoints = 2400; % number of data points
ntotal = 6; % number of variables

%-----
% this code was adapted from the example provided by Villaverde et al.
% MI MIDER OPTIONS
% Entropic parameter:
options.q = 1; % q = 1 (Boltzmann-Gibbs entropy) | q > 1 (Tsallis entropy)

% Normalization of the mutual information (MI)
options.MItype = 'MIlicheals'; % 'MI' | 'MIichaels' | 'MIlinfoot' | 'MIstudholme'

% Adaptive estimation of MI -> Partition the joint space of X,Y so that the
% fraction of occupied bins with >= 5 points is at least = options.fraction:
options.fraction = 0.1*(log10(npoints)-1);
if options.fraction < 0.01, options.fraction = 0.01; end %lower bound=0.01

% Maximum time lag considered (> 0):
options.taumax = 1;

% Number of entropy reduction (ERT) rounds to carry out (0, 1, 2, or 3):
options.ert_crit = 2;

% Entropy reduction threshold. Enter a number between 0.0 and 0.2 to fix it
% manually, or choose 'adapt' to use a value obtained from the data:
options.threshold = 'adapt';
```

```

% Plot MI arrays (=1) or not (=0):
options.plotMI = 1;
%-----
% RUN MIDER
s = SUBJECT_#; % subject of interest
for b = 1:numel(bands)% frequency band
    data = FB_Data(s).(bands{b});
    for z = 1:30% all trials
        temp = data(:, :, z);
        loc = 2401;      nseg = 2400;      noverlap = 600;

        for segment = 1:19 % segment EMG data for MI to be ran on
            if segment == 1
                start = 1;
                Mimat(:, :, segment) = temp(start:start+nseg-1, :);
            else
                start = loc - noverlap;
                Mimat(:, :, segment) = temp(start:start+nseg-1, :);
                loc = start + nseg;
            end
        end

        for segment = 1:19% run MI on EMG segments
            x = Mimat(:, :, segment);
            Output = mider(x, options);
            temp = Output.MIm;% select normalized MI
            values = temp(:, :, 1);

            % identify pairs of interest from MIDER output
            pairs(:, segment) = values([3 5 17 10 12 24 2 16 30]);
        end
        MIavg(:, z) = mean(pairs, 2);
    end
    FB_MI.(bands{b}) = MIavg;
end

for b = 1:numel(bands)
    Temp_SB(s).(bands{b}) = FB_MI.(bands{b});
end
save('Temp_SB_MI_m.mat', 'Temp_SB');% save MI

```

Bibliography

- [1] D. Winter, “Human balance and posture control during standing and walking,” *Gait & Posture*, vol. 3, no. 4, pp. 193–214, Dec. 1995.
- [2] A. S. Pollock, B. R. Durward, P. J. Rowe, and J. P. Paul, “What is balance?,” *Clinical Rehabilitation*, vol. 14, no. 4, pp. 402–406, Aug. 2000.
- [3] Y. Ivanenko and V. S. Gurfinkel, “Human Postural Control,” *Frontiers in Neuroscience*, vol. 12, 2018.
- [4] F. B. Horak, “Postural orientation and equilibrium: what do we need to know about neural control of balance to prevent falls?,” *Age and Ageing*, vol. 35, no. suppl_2, pp. ii7–ii11, Sep. 2006.
- [5] P. Morasso, A. Cherif, and J. Zenzeri, “Quiet standing: The Single Inverted Pendulum model is not so bad after all,” *PLOS ONE*, vol. 14, no. 3, p. e0213870, 2019.
- [6] C. J. De Luca and Z. Erim, “Common Drive in Motor Units of a Synergistic Muscle Pair,” *Journal of Neurophysiology*, vol. 87, no. 4, pp. 2200–2204, Apr. 2002.
- [7] V. Krishnamoorthy, M. L. Latash, J. P. Scholz, and V. M. Zatsiorsky, “Muscle synergies during shifts of the center of pressure by standing persons,” *Experimental Brain Research*, vol. 152, no. 3, pp. 281–292, Oct. 2003.
- [8] G. Mochizuki, J. G. Semmler, T. D. Ivanova, and S. J. Garland, “Low-frequency common modulation of soleus motor unit discharge is enhanced during postural control in humans,” *Experimental Brain Research*, vol. 175, no. 4, pp. 584–595, Nov. 2006.
- [9] M. Saffer, T. Kiemel, and J. Jeka, “Coherence analysis of muscle activity during quiet stance,” *Experimental Brain Research; Heidelberg*, vol. 185, no. 2, pp. 215–26, Feb. 2008.
- [10] T. W. Boonstra, M. Roerdink, A. Daffertshofer, B. van Vugt, G. van Werven, and P. J. Beek, “Low-Alcohol Doses Reduce Common 10- to 15-Hz Input to Bilateral Leg Muscles During Quiet Standing,” *Journal of Neurophysiology*, vol. 100, no. 4, pp. 2158–2164, Oct. 2008.
- [11] E. H. F. van Asseldonk, S. F. Campfens, S. J. F. Verwer, M. J. A. M. van Putten, and D. F. Stegeman, “Reliability and Agreement of Intramuscular Coherence in Tibialis Anterior Muscle,” *PLOS ONE*, vol. 9, no. 2, p. e88428, Feb. 2014.
- [12] A. Danna-Dos-Santos *et al.*, “Multi-muscle control during bipedal stance: an EMG-EMG analysis approach,” *Experimental Brain Research*, vol. 232, no. 1, pp. 75–87, Jan. 2014.
- [13] H. Obata, M. O. Abe, K. Masani, and K. Nakazawa, “Modulation between bilateral legs and within unilateral muscle synergists of postural muscle activity changes with development and aging,” *Experimental Brain Research*, vol. 232, no. 1, pp. 1–11, Jan. 2014.

- [14] A. Danna-Dos-Santos *et al.*, “The influence of visual information on multi-muscle control during quiet stance: a spectral analysis approach,” *Experimental Brain Research; Heidelberg*, vol. 233, no. 2, pp. 657–669, Feb. 2015.
- [15] T. W. Boonstra, A. Danna-dos-santos, H. Xie, M. Roerdink, J. F. Stins, and M. Breakspear, “Muscle networks: Connectivity analysis of EMG activity during postural control,” *Scientific Reports (Nature Publisher Group); London*, vol. 5, p. 17830, Dec. 2015.
- [16] X. García-Massó, M. Pellicer-Chenoll, L. M. Gonzalez, and J. L. Toca-Herrera, “The difficulty of the postural control task affects multi-muscle control during quiet standing,” *Experimental Brain Research*, vol. 234, pp. 1977–1986, 2016.
- [17] A. M. Degani, C. T. Leonard, and A. Danna-Dos-Santos, “The use of intermuscular coherence analysis as a novel approach to detect age-related changes on postural muscle synergy,” *Neurosci. Lett.*, vol. 656, pp. 108–113, Aug. 2017.
- [18] T. Nandi, T. Hortobagyi, H. G. van Keeken, G. J. Salem, and C. J. C. Lamoth, “Standing task difficulty related increase in agonist-agonist and agonist-antagonist common inputs are driven by corticospinal and subcortical inputs respectively,” *Scientific Reports*, vol. 9, p. 2439, Feb. 2019.
- [19] J. N. Kerkman, A. Daffertshofer, L. L. Gollo, M. Breakspear, and T. W. Boonstra, “Network structure of the human musculoskeletal system shapes neural interactions on multiple time scales,” *Science Advances*, vol. 4, no. 6, p. eaat0497, Jun. 2018.
- [20] P. Grosse, M. J. Cassidy, and P. Brown, “EEG-EMG, MEG-EMG and EMG-EMG frequency analysis: physiological principles and clinical applications,” *Clin Neurophysiol*, vol. 113, no. 10, pp. 1523–1531, Oct. 2002.
- [21] D. Farina, R. Merletti, and R. M. Enoka, “The extraction of neural strategies from the surface EMG: an update,” *Journal of Applied Physiology*, vol. 117, no. 11, pp. 1215–1230, Dec. 2014.
- [22] A. Ojha, “Analysis of Coherence between Electromyographic (EMG) signals to Examine Neural Correlations in Muscular Activation during Standing Balance Tasks: A Pilot Study,” Grand Valley State University, Grand Rapids, 2018.
- [23] R. Chiba, K. Takakusaki, J. Ota, A. Yozu, and N. Haga, “Human upright posture control models based on multisensory inputs; in fast and slow dynamics,” *Neuroscience Research*, vol. 104, pp. 96–104, Mar. 2016.
- [24] N. Bernstein, *The Co-Ordination and Regulation of Movements*, 1st ed. Oxford, New York: Pergamon Press, 1967.
- [25] Z. Wang, J. H. Ko, J. H. Challis, and K. M. Newell, “The degrees of freedom problem in human standing posture: collective and component dynamics,” *PLOS ONE*, vol. 9, no. 1, p. e85414, 2014.
- [26] M. Bruton and N. O’Dwyer, “Synergies in coordination: a comprehensive overview of neural, computational, and behavioral approaches,” *Journal of Neurophysiology*, vol. 120, no. 6, pp. 2761–2774, Oct. 2018.

- [27] D. R. Brillinger and A. Guha, “Mutual information in the frequency domain,” *Journal of Statistical Planning and Inference*, vol. 137, no. 3, pp. 1076–1084, Mar. 2007.
- [28] A. F. Villaverde, J. Ross, F. Morán, and J. R. Banga, “MIDER: network inference with mutual information distance and entropy reduction,” *PLoS ONE*, vol. 9, no. 5, p. e96732.
- [29] C. E. Shannon, “A Mathematical Theory of Communication,” *Bell System Technical Journal*, vol. 27, no. 3, pp. 379–423, 1948.
- [30] G. S. Michaels, D. B. Carr, M. Askenazi, S. Fuhrman, X. Wen, and R. Somogyi, “Cluster analysis and data visualization of large-scale gene expression data,” *Pac Symp Biocomput*, pp. 42–53, 1998.
- [31] J. P. Scholz and G. Schöner, “The uncontrolled manifold concept: identifying control variables for a functional task,” *Exp Brain Res*, vol. 126, no. 3, pp. 289–306, May 1999.
- [32] M. L. Latash, J. P. Scholz, and G. Schöner, “Motor control strategies revealed in the structure of motor variability,” *Exerc Sport Sci Rev*, vol. 30, no. 1, pp. 26–31, Jan. 2002.
- [33] M. W. Rogers and M.-L. Mille, “Balance perturbations,” *Handbook of Clinical Neurology*, vol. 159, pp. 85–105, 2018.
- [34] “Materials for Healthcare Providers | STEADI - Older Adult Fall Prevention | CDC Injury Center,” 05-Feb-2019. [Online]. Available: <https://www.cdc.gov/steady/materials.html>. [Accessed: 14-Jun-2019].
- [35] M. G. Carpenter, C. D. Murnaghan, and J. T. Inglis, “Shifting the balance: evidence of an exploratory role for postural sway,” *Neuroscience*, vol. 171, no. 1, pp. 196–204, Nov. 2010.
- [36] T. Yamamoto *et al.*, “Universal and individual characteristics of postural sway during quiet standing in healthy young adults,” *Physiological Reports*, vol. 3, no. 3, Mar. 2015.
- [37] M. J. Warnica, T. B. Weaver, S. D. Prentice, and A. C. Laing, “The influence of ankle muscle activation on postural sway during quiet stance,” *Gait & Posture*, vol. 39, no. 4, pp. 1115–1121, Apr. 2014.
- [38] M. B. I. Raez, M. S. Hussain, and F. Mohd-Yasin, “Techniques of EMG signal analysis: detection, processing, classification and applications,” *Biological Procedures Online*, vol. 8, pp. 11–35, Mar. 2006.
- [39] C. J. Cellucci, A. M. Albano, and P. E. Rapp, “Statistical validation of mutual information calculations: Comparison of alternative numerical algorithms,” *Phys. Rev. E*, vol. 71, no. 6, p. 066208, Jun. 2005.